

NATIONAL TRANSPORTATION SAFETY BOARD

Office of Research and Engineering
Washington, D.C. 20594

October 1, 2003

Aircraft Performance

Group Chairman's Aircraft Performance Study Addendum #1 by John O'Callaghan

ABSTRACT

This Addendum to the *Aircraft Performance Study*¹ introduces corrections to the pitch, roll, and heading angles recorded on the Flight Data Recorder (FDR) to account for latency and filtering effects in the aircraft computers that process the data prior to its being recorded. The effect of these corrections on the sideslip angle computed by integrating the recorded accelerations is also described. Finally, the Addendum presents the results of NTSB simulations of the accident event, incorporating external pitching, rolling, and yawing moments that can be attributable to a wake encounter. The effect of the external moments on the aircraft with no control inputs is evaluated, as is the effect of a yaw damper design that is always capable of attenuating rudder deflections commanded by pedal deflection.

A correction to Figure #8 in the *Aircraft Performance Study* is also provided.

1. INTRODUCTION

1.1. Accident Identification

Location:	Belle Harbor, New York
Date:	November 12, 2001
Time:	09:17 AM Eastern Standard Time (EST)
Flight:	American Airlines Flight 587
Aircraft:	Airbus A300B4-605R, Registration N14053
NTSB#:	DCA02MA001

¹ O'Callaghan, J., *Aircraft Performance Group Chairman's Aircraft Performance Study for American Airlines Flight 587 (DCA02MA001)*, National Transportation Safety Board, October 10, 2002.

1.2 Aircraft Performance Group Members

Chairman: John O'Callaghan
 National Resource Specialist - Aircraft Performance
 National Transportation Safety Board (NTSB)
 490 L'Enfant Plaza E, SW
 Washington, DC 20594

Members: Dominique Buisson
 Senior Expert – Flight Operations
 Engineering – Systems and Integration Tests Center
 Airbus
 1 Rond Point Maurice Bellonte
 31707 Blagnac Cedex, France

Captain Jerry Mumfrey
 F100/A300 Technical Pilot, Flight Operations Technical
 American Airlines
 4601 Highway 360
 Fort Worth, Texas 76155

Steven O'Neal
 Flight Test Engineer
 Federal Aviation Administration (FAA)
 Seattle Aircraft Certification Office, ANM-160S
 1601 Lind Avenue, S.W.
 Renton, Washington 98055-4056

Yann Torres
 Investigator – Engineering Department
 Bureau Enquetes - Accidents (BEA)
 Bâtiment 153 - Aéroport du Bourget
 93352 Le Bourget Cedex, France

1.3 Accident Summary

On November 12, 2001, at approximately 9:17 AM Eastern Daylight Time (EDT), American Airlines flight 587 (AAL587), an Airbus Industrie A300-600, was destroyed when it crashed into a residential area of Belle Harbor, New York, shortly after takeoff from runway 31L at John F. Kennedy International Airport (JFK), Jamaica, New York. Before impact, the vertical stabilizer, rudder, and left and right engines departed the airplane. The 2 pilots, 7 flight attendants, 251 passengers, and 5 persons on the ground were killed. Visual meteorological conditions prevailed and an instrument flight rules flight plan had been filed for the flight destined for Santo Domingo, Dominican Republic. The scheduled passenger flight was conducted under 14 *Code of Federal Regulations* (CFR) Part 121.

1.4. Data Latency Corrections

Section D-IV of the *Aircraft Performance Study* presents the Euler angles (pitch, roll, and heading) recorded on the FDR, and describes how these are used along with the recorded load factor data and other recorded parameters to obtain an inertial position of the airplane in time. Time-accurate Euler angles are required to calculate the airplane accelerations and velocities in the body axis system, and to perform coordinate transformations between the body axis system and the Earth axis system. In the *Aircraft Performance Study*, no corrections are made to the recorded Euler angles: the recorded data is used to describe the attitude of the airplane at the time associated with each recorded value. Subsequent investigation has revealed that the time associated with the recorded DFDR Euler angles can be delayed in time relative to other DFDR parameters, which introduces errors into computations that use both the delayed Euler angles and other, non-delayed parameters as inputs. If the magnitude of the delays in the Euler angles is known, the delays can be corrected and the correct time relationship of the Euler angles to the other parameters determined².

Section 2.1 of this Addendum describes adjustments to the recorded Euler angle data to correct for recording latencies, and Section 3.1 presents new sideslip angle data computed using the corrected Euler angles. The uncertainty in the sideslip angle calculation and resulting tail loads associated with various combinations of the full range of possible data latency values is still under investigation.

1.5. NTSB Simulations of Final Seconds of Flight

Section D-V of the *Aircraft Performance Study* presents the results of an Airbus Industrie simulation of the accident sequence. Section 2.2.1 of this Addendum describes a similar NTSB simulation of the accident sequence, that uses a slightly different approach to account for the aerodynamic effects of the wake encounter and external winds. The results of this simulation are presented in Section 3.2.1. The effects of the wake encounter and winds alone - without any accompanying control inputs - are also shown. Finally, a simulation of the accident sequence incorporating an alternative yaw damper design, in which the yaw damper inputs can not be overridden by pilot pedal deflections at the rudder limits, is described in Section 2.2.2. The results of this simulation are presented in Section 3.2.2.

² There is always a certain time delay between the sensing and the recording of any parameter, because of the time required to acquire, process, and store electronic signals. If the delay is the same for every sample of all the DFDR parameters, then all the recorded data will be synchronized and the value of any parameter corresponding to the same instant in time as the value of another parameter can be determined. When the delays vary from sample to sample or from parameter to parameter, the data is no longer synchronized.

2. METHOD

2.1. Data Latency Corrections

The sources and magnitudes of the delays in the recorded Euler angles and other parameters are described in Reference 1³. Table 1 from Reference 1 lists the potential delays in the Euler angles as follows:

Parameter	Potential Latency (ms)
Pitch angle	80 to 150
Roll angle	80 to 150
Magnetic Heading	170 to 320

The latency for any given parameter is not necessarily constant from sample to sample. For example, one sample of Magnetic Heading could be recorded only 170 ms after it was sensed, but the next sample could be recorded 320 ms after it was sensed. Thus, the recorded time between the two samples could be in error by as much as $320 - 170 = 150$ ms⁴. This error in the times associated with Heading will propagate into the values of parameters that are calculated using this time, such as yaw rate. There is no way to correct for this error exactly because the actual latency associated with each sample is undetermined; all that is known is that it lies in a certain range.

The maximum latency for Pitch and Roll is 150 ms, and the minimum latency for Magnetic Heading is 170 ms, so if no latency corrections are made, Pitch and Roll will be out of phase with Magnetic Heading by at least 20 ms. If Pitch and Roll are at their minimum latency (80 ms) and Magnetic Heading is at its maximum latency (320 ms), these parameters would be out of phase by 240 ms.

Reference 1 indicates that the latency for some other parameters - such as the recorded cockpit control positions, and three-axis accelerometer data - is only about 20 ms. Without any corrections, then, Pitch and Roll will be out of phase with the cockpit controls and load factors by 60 to 130 ms, and Magnetic Heading will be out of phase with these parameters by 150 to 300 ms.

The errors in the time relationships between the recorded parameters introduced by these latencies are small, but they can become significant when analyzing fast, dynamic maneuvers requiring precise timing of critical events. Such is the case in the AAL587 accident, where identifying the moment of tail separation, and defining the flight condition and structural loads on the tail at that point, is of interest. At the time the tail separated, the airplane was yawing to the left at about 8 degrees/second, and the sideslip angle was increasing at about the same rate. Thus, a 125 ms uncertainty in time can lead to a $(0.125 \text{ sec}) \times (8 \text{ deg/sec}) = 1$ degree uncertainty in sideslip angle, which is significant in terms of loads on the tail.

³ In this Addendum, "delay" and "latency" are used interchangeably, and include the effects of computer processing times, parameter filtering, and parameter refresh rates. See Reference 1 for details.

⁴ If the computers involved in the processing of the FDR data are in a stable operating configuration, the statistical probability of a change in latency from the minimum possible value to the maximum possible value over one sample is very low. However, such a variation is impossible to rule out.

Since the actual latency for each sample of each parameter is undetermined, in this Addendum corrections to the Euler angle data have been made assuming that the sample-to-sample latency for each parameter is constant, and that its value lies near the middle of the range identified in Reference 1⁵:

Latency for Pitch and Roll: 125 ms
 Latency for Magnetic Heading: 250 ms

To correct for these (assumed) latencies, the time associated with each FDR sample of pitch, roll, and heading data is adjusted by the value of the latency, as follows:

$$t_c = t_{\text{FDR}} - t_l$$

where t_c = the sample time corrected for the latency, t_{FDR} = the uncorrected FDR time associated with the sample, and t_l = the latency value.

Section D-IV of the *Aircraft Performance Study* describes how the recorded FDR data, including the Euler angles, are used to derive additional flight parameters, such as the sideslip angle. The sideslip angle calculation was repeated with the latency-corrected Euler angle data, resulting in the changes presented in Section 3.1.

2.2. NTSB Simulations of Final Seconds of Flight

Section V of the *Aircraft Performance Study* describes a simulation of the final seconds of the accident flight conducted by Airbus Industrie⁶. Since the publication of the *Aircraft Performance Study*, the NTSB has developed a desktop simulation of the A300-600 using simulator model data provided by Airbus⁷. An NTSB simulator match of the last seconds of the flight, which uses external moments as well as wind gusts to account for the effects of the airplane's encounter with a wake vortex, is presented in Section 2.2.1. Section 2.2.2. shows the effect that a pedal limiter, which prevents pilot inputs from overriding yaw damper commands at the rudder limits, would have on the accident sequence.

2.2.1. NTSB Simulator Match of Accident Sequence

As discussed in the *Aircraft Performance Study*, crew comments recorded on the CVR, a NASA analysis of the wake of the Boeing 747 that departed JFK ahead of AAL587, and the AAL587 FDR data all indicate that AAL587 encountered the 747 wake twice shortly before the accident. The Airbus and NTSB simulations of the accident start just before the second wake encounter, at about 09:15:47 EST.

As described in Appendix B to the *Aircraft Performance Study*, the trailing vortices in the wake of the B747 produce significant disturbances in the direction and velocity of the surrounding air. In fact, the vortices may induce updrafts of 20 knots in one place, and

⁵ The uncertainty in the sideslip angle calculation and resulting tail loads associated with various combinations of the full range of data latency values is still under investigation.

⁶ Airbus has updated their simulation of the accident sequence since the publication of the *Aircraft Performance Study*. The latest Airbus simulation incorporates a lateral wind gust, as well as a vertical wind gust, near the time of the right wheel and pedal inputs, resulting in a better match of computed sideslip angle.

⁷ Simulations in general, and "desktop simulations" in particular, are described in Section V of the *Aircraft Performance Study*.

downdrafts of 20 knots only 30 feet away. Similar differences in horizontal gusts are also possible. Depending on the geometry of how the airplane encounters the wake, these changes in wind speed and direction can cause the angle of attack to increase on one wing and decrease on the other, creating a rolling moment. Changes in the local flow angles over the horizontal stabilizer can produce pitching moments, and changes in flow over the vertical stabilizer can produce yawing moments. These “vortex-induced” rolling, pitching, and yawing moments are not modeled in the baseline A300 simulator,⁸ and so if they not accounted for in some way, the simulator will not be able to duplicate all the forces and moments acting on the actual airplane, and the simulator motion will not match that recorded on the FDR.

The load factor and engine N1 data fluctuations recorded on the FDR between about 09:15:50 and 09:15:54 suggest that the second wake encounter occurred during this time, and that the motion of the airplane was affected by the wind gusts induced by the wake. To account for these effects, during this 4 second period the NTSB simulation incorporates external rolling, pitching, and yawing moments that make the simulator motion more closely match the motion recorded on the FDR. After the 4 second period, the airplane is assumed to be free of the wake, and the external moments are removed.

In addition to external moments, the wake can induce forces on the airplane that can be accounted for by changes in the velocity of the airmass surrounding the airplane (as opposed to differential changes in the flow at various points). These gross effects are modeled in the simulator as vertical wind gusts and changes in the horizontal wind speed and direction.

Throughout the simulation, the simulator cockpit control positions and aerodynamic surface positions are driven so as to match the positions recorded on the FDR⁹ as closely as possible without sacrificing the match of the motion recorded by the FDR. Because of the effects of the SDAC filter (see Section D-IV of the *Aircraft Performance Study*), the *filtered* simulator control surface positions are matched to the FDR positions.

To get a sense of the magnitude of the effects of the vortex-induced external moments and vertical and horizontal wind gusts, the simulator match is repeated, but without any cockpit control or control surface movements. The simulator then computes the response of the airplane solely to the forces and moments induced by the wake encounter. The results of this simulation, together with the simulator match described above, are presented in Section 3.2.1.

⁸ The baseline simulator model can account for external wind gusts (changes in the vertical and horizontal wind), but not does not include a model for arbitrary external forces and moments exerted on the airplane such as those that can be produced by a wake vortex encounter.

⁹ In this study, only the FDR Euler angles are adjusted for data latency. The potential latency on the cockpit control positions is minimal (20 ms), and the error in the control surface position data is dominated by the effects of the SDAC filter (see pp. 19-20 of the *Aircraft Performance Study*).

2.2.2. Evaluation of the Effect of a Pedal Limiter

The Rudder Travel Limiter Unit (RTLUL) system of the A300-600 limits the amount of rudder deflection available at various airspeeds. Both the rudder pedals and the yaw damper system can command rudder input, but the sum of these commands is restricted to the limit imposed by the RTLUL. Consequently, if the yaw damper is commanding a left rudder deflection, the right rudder pedal command available to the pilot will be greater than the value of the RTLUL limit, and the available left rudder pedal command will be less than the RTLUL limit. In both cases, however, the sum of the available pedal command and yaw damper command will equal the RTLUL limit (see Figure 1a).

This implementation allows the pilot to “override” the yaw damper at the rudder travel limits. For example, if the RTLUL limit is 10° , and the pilot commands full right pedal, the pedal will move until 10° of right rudder is obtained (corresponding to a pedal deflection of about $(10^\circ \text{ rudder}) \times (0.7 \text{ pedal/rudder}) = (7^\circ \text{ pedal})$). If the yaw damper then commands 2° of left rudder, the rudder will back off to 8° . Since the rudder limit is 10° , 2 additional degrees of rudder are now available to the pilot. He can now deflect the pedal an additional $2^\circ \times (0.7) = 1.4^\circ$, to 8.4° , resulting in 12° of right rudder commanded by the pedal. The sum of the rudder commands from the pedal and yaw damper are $12^\circ \text{ right} + 2^\circ \text{ left} = 10^\circ \text{ right}$, the RTLUL limit.

Since the rudder authority available from the pedals is higher than the authority available to the yaw damper, the pilot will always be able to keep the rudder at the RTLUL limit by applying the necessary (increasing) pressure to the rudder pedals, thereby overriding yaw damper commands that would move the rudder towards neutral. The square wave-like rudder inputs shown in the Airbus and NTSB simulations, which are consistent with the (filtered) FDR rudder data, suggest that this suppression of the yaw damper inputs at the rudder limits probably occurred during the accident flight.

Since the yaw damper acts to attenuate directional oscillations such as the Dutch Roll mode (thereby suppressing the dynamic buildup of the sideslip angle), it is of interest to determine what effect on the aircraft motion and loads the yaw damper commands would have if they could not be overridden at the rudder limits by pedal inputs. In this implementation, the rudder available to be commanded by pedal, as well as the sum of the pedal and yaw damper commands, is restricted to the RTLUL limit (see Figure 1b). With full pedal input and the rudder at the RTLUL limit, the yaw damper could move the rudder back towards neutral, but this would not free up additional pedal motion with which to command the rudder back to the rudder limit. In effect, the pedal, as well as the rudder, is limited, and this implementation can be considered a “Pedal Limiter” system.

The effects of a Pedal Limiter were evaluated by driving the simulator match described in Section 2.2.1 with pedal (instead of rudder position directly), and allowing the simulation to compute the rudder resulting from the pedal command and the yaw damper, accounting for both the RTLUL and a Pedal Limiter. The pedal used in the simulation was chosen so as to result in the rudder position used in the original simulator match, if yaw damper inputs are ignored. The results of this simulation are presented in Section 3.2.2.

3. RESULTS

3.1. Data Latency Corrections

The Euler angles adjusted for data time latencies as described in Section 2.1 are shown in Figure 2, along with the unadjusted FDR data¹⁰. The sideslip angle calculated using the adjusted Euler angles is shown in Figure 3. The original sideslip angle, computed without any adjustments to the Euler angles, is also shown. Not surprisingly, the effect of the 250 ms adjustment to Magnetic Heading is to advance the computed sideslip angle in time by about a quarter second. As a result, at the approximate time of the tail separation (about coincident with the “loud bang” sound recorded on the CVR), the updated sideslip angle is about 2° higher than the original. The uncertainty in the sideslip angle calculation and resulting tail loads associated with various combinations of the full range of possible data latency values is still under investigation.

3.2.1. NTSB Simulator Match of Accident Sequence

Match Using Cockpit Controls and Vortex Effects

The results of the NTSB simulator match of the final seconds of flight are shown in Figures 4a-4h. The results are shown as a function of elapsed time; an elapsed time of 839 sec. corresponds to an ATC time of 09:16:47.2 EST. No simulator results are shown beyond time 850.3 (09:15:58.5 EST), corresponding to the “sound of loud bang” recorded on the Cockpit Voice Recorder. After this time, the vertical tail is separated from the accident airplane and the simulator (which retains its tail) no longer models the actual aerodynamics of the damaged airplane.

The results of the same simulation run without cockpit control inputs are shown in Figures 5a-5h in order to illustrate the effect of the wake vortex encounter on the airplane.

Figure 4a presents the cockpit control positions and control surface positions used to drive the simulation. The rudder and elevator surface positions were driven directly (as opposed to through the cockpit controls). The rudder position used is the same as that used by Airbus in their simulations of the accident, as presented in the *Aircraft Performance Study*¹¹. As shown in Figure 4a, when this rudder position is filtered, it matches closely the rudder position recorded by the FDR.

The wheel position shown in Figure 4a was used to command the spoilers and ailerons. The resulting aileron positions are also shown in the Figure. The filtered aileron positions are shown for comparison with the FDR recorded aileron positions. Between time 842 and 846, where the external moments are active (see Figure 4c), the wheel matches the FDR wheel very well because the external rolling moment keeps the simulator bank angle in good agreement with the FDR bank angle. During this time, all the effects that would cause imperfections in the match (the vortex effects, approximations and uncertainties in the simulator aerodynamic and flight control models, etc.) are lumped into the “vortex effects”

¹⁰ Only the last 11 seconds of recorded data are shown, so that the effect of the small time adjustment can be seen on the scale of the plots. This time period starts just prior to the second wake encounter.

¹¹ Since the publication of the *Aircraft Performance Study*, Airbus has updated their simulation to include a lateral gust to help account for wake vortex effects. The rudder position used in the updated simulation is the same as that used in Simulation #11, presented in the *Study*.

category and accounted for by the external rolling moment. After time 846, it is assumed that the airplane is free of external influences, and so the external moments are not available to correct for imperfections in the simulator models. As a result, the simulator match of wheel is not as good; for example, the large wheel excursions recorded on the FDR at times 847.3 and 848.3 are not matched perfectly by the simulator. It is likely that part of the error lies in the simulator modeling of the relationship between the wheel and the spoilers and ailerons, because the filtered simulator aileron positions match the FDR positions well, indicating that the simulator response to ailerons is similar to that recorded by the FDR (note the excellent match of the FDR bank angle, shown in Figure 4e).

The bottom graph of Figure 4a shows the simulator elevator and stabilizer, and the filtered simulator elevator compared to the FDR. The FDR points in Figure 4a have been shifted about 2° trailing edge up, to match the simulator elevator at the trimmed initial condition. It is improbable that the real airplane was in a trimmed climb with 2° of elevator, and more likely that the elevator was actually near neutral, as required by the simulator. The non-zero elevator in the FDR data may be due to an offset in the elevator position sensor (such offsets are not uncommon).

From time 842 to 846 the filtered simulator elevator matches the (shifted) FDR data very well; this is possible because during this time the external pitching moment corrects for vortex effects and imperfections in the simulator model, ensuring a good match of the FDR pitch angle (see Figure 4e). After time 846, the external pitching moment is zero, and to maintain a good match of pitch angle, an elevator is required that does not match the FDR perfectly. Nonetheless, the shape of the elevator trace matches the FDR, and in many places the values of the elevator deflection are in excellent agreement with the FDR.

Figure 4b shows the thrust used to drive the simulation. The simulator engine N1 values are forced to match those recorded on the FDR, and then actual thrust is computed in the simulator using a simplified engine model. Note that the right engine is at a slightly higher thrust than the left engine. This creates a small yawing moment that, if not countered somehow, causes the simulator to deviate from the recorded FDR heading during the turn shortly before the second wake encounter. To balance this thrust asymmetry, a small external yawing moment (equivalent to less than 1° of rudder) is required in the simulator. After the wake encounter, this external moment is no longer required (see Figure 4c).

The external pitching (ΔC_M), rolling (ΔC_R), and yawing (ΔC_N) moments used in the simulation are shown in Figure 4c. Note that all three become active shortly after time = 842 sec., and become inactive by time = 846 sec., consistent with the period during which the wake vortex is assumed to have an effect on the airplane. The external pitching moment is tailored so as to match the FDR pitch angle, the rolling moment is tailored so as to match the FDR bank angle, and the yawing moment is tailored so as to match the FDR heading angle. Note that these external moments all show an abrupt effect in one direction, followed by a sudden reversal of the effect in the opposite direction. The effects of these moments on the airplane motion, without any influence from control inputs, is shown in the simulator results plotted in Figures 5a-5h, discussed below.

Figure 4d shows the external winds used in the simulation. The small variations in horizontal wind are tailored to match airspeed, and the vertical wind is tailored to match angle of attack and vertical load factor. Note that the large vertical gust in Figure 4d occurs between time = 842 and 846, consistent with the wake vortex encounter.

Figure 4e shows the simulator match of the FDR Euler angles, together with a cubic spline interpolation through the FDR data points.¹² The simulator is in good agreement with the FDR, indicating that the control movements, thrust, and external moments and winds used to drive the simulation properly account for the airplane's motion.

The differences between the simulator results that pass through the recorded FDR points, and the cubic spline interpolation through the same points, indicate that the 1 Hz sample rate of the Euler angles allows some uncertainty in defining the attitude of the airplane throughout a very dynamic maneuver. In particular, the differences between the interpolated and simulator heading between time 847.5 and 849 result in differences between the calculated sideslip angle and the simulator sideslip angle, which can be significant in terms of load on the vertical tail.

The angle of attack and sideslip angle results are shown in Figure 4f. The simulator match of angle of attack is not as good as that of other parameters, though it is still within about 1.5° of the recorded vane angle of attack.¹³ A filtered angle of attack is also shown; the filter applied is the same SDAC filter applied to the control surface parameters, defined in Section D-IV of the *Aircraft Performance Study*. While it is known that the angle of attack from the vane measurement is processed and filtered, it is not clear that the filter that applies is indeed the same as that applied to the control surfaces; furthermore, there may be dynamics associated with the mass of the vane itself that produce some uncertainty or error in the actual angle of attack measurement. These issues should be considered when evaluating the angle of attack results.

The simulator sideslip angle and the sideslip angle computed from the integration of the FDR accelerometer and Euler angle data are compared in the bottom graph of Figure 4f.¹⁴ The differences mirror the differences between the simulator and interpolated heading angles shown in Figure 4e, and underscore the effect of the low sample rate of the Euler angles on the sideslip calculation.

Figure 4g compares the simulator load factors at the CG with those recorded on the FDR, and to the FDR data corrected for bias and accelerometer location, as described in Section D-IV of the *Aircraft Performance Study*.¹⁵

Finally, Figure 4h shows the match of pressure altitude and airspeed. Note that the simulator altitude agrees very well with the altitude computed from the accelerometer integration, which differs substantially from the recorded FDR pressure altitude. This result illustrates the unreliability of the pressure based altitude data in areas of very dynamic maneuvering and high sideslip, and validates the calculations based on the integration of the accelerometer data.

¹² The FDR Euler angles plotted in Figure 4e have been adjusted for data latencies, as described in Section 2.1 and shown in Figure 2.

¹³ A measure of the quality of a simulator match is provided by AC-12040B, "Airplane Simulator Qualification," which defines acceptable tolerances on the agreement between simulator and flight test parameters for various maneuvers required for the certification of flight simulators. The tolerance on angle of attack, where required, is usually 1.5°.

¹⁴ The Euler angles used in the sideslip angle calculation are those adjusted for time latencies.

¹⁵ The CG position assumed in the simulator is at 28% Mean Aerodynamic Chord, on the airplane centerline, 0.713 meters (2.34 ft.) below the fuselage reference line. The accelerometers are assumed to be 2.89 ft. in front of, 1.54 ft. to the right of, and 0.07 ft. below the CG.

Match Using Vortex Effects Only - No Control Inputs

The effects of the forces and moments generated by the wake encounter on the airplane motion can be evaluated by repeating the simulator match described above, but without any control surface inputs. The airplane is trimmed in a climbing right turn as before, but throughout the simulation the controls are held at these trim positions, so that the only deviation from the trim condition is the result of the wake encounter. The results of this “vortex only” simulation are shown in Figures 5a-5h.

Figure 5a shows the control surface positions. As just described, they are held fixed at their trim positions throughout the simulation.

Figures 5b-5d show that the thrust, external moments, and winds used are the same as in the previous simulation.

Figure 5e shows the result of the wake encounter on the Euler angles. The abrupt increase in the pitch angle at time 844 is absent, which results in the pitch angle being about 2° to 4° lower after the wake encounter than in the previous simulation.

The effect of the external rolling moment is to initially roll the aircraft further to left, from about -24° to -34° . Following this 10° excursion, the rolling moment rolls the airplane back to the right to -24° , and thereafter, with the external rolling moment at zero after time 846, the bank angle slowly increases up to -36° before starting to roll slowly back towards the right. The roll rate during the first 10° roll excursion to the left is about 9.2 degrees/sec.

The effect of the external yawing moment on heading is relatively slight - the heading angle decreases steadily, consistent with the left bank angle, with some slight undulations as a result of the wake encounter. The difference in the heading trace compared to the previous simulation is dramatic, indicating that the large heading oscillations present in that simulation are a result of the rudder movements.

The angle of attack and sideslip angle from the “vortex only” simulation are shown in Figure 5f. Note that the sideslip excursions resulting from the wake encounter are less than 2.5° , indicating, again, that the large sideslip buildup in the previous simulation is the result of the rudder movements.

The load factor results are shown in Figure 5g, and indicate that while the first large drop in normal load factor is the result of the vertical gust induced by the wake encounter, the subsequent large oscillations in normal and lateral load factors are the result of control surface movements.

Figure 5h shows the altitude and airspeed resulting from the “vortex only” match. Consistent with the lower pitch angle in this simulation, the altitude is lower and the airspeed higher than previously.

3.2.2. Evaluation of the Effect of a Pedal Limiter

The results of the pedal limiter simulation described in Section 2.2.2 are presented in Figures 6a-6j.

Figures 6a and 6b show the controls used to drive the simulation. The top graph in Figure 6a shows the rudder position resulting from the pedal inputs and yaw damper commands shown in Figure 6b. Note that, as expected, preventing the pedal from overriding the yaw damper at the rudder limits results in a reduction in the rudder deflection. The wheel and elevator positions used in this simulation are identical to those used previously.

The pedal input shown in Figure 6b was chosen so as to closely match the rudder deflection used in the previous simulations, assuming the yaw damper command is zero. The resulting no-yaw-damper-input rudder and airplane motion is shown in Figures 6a-6j as the “Simulator, with yaw damper override” curves. These results are not identical to the results shown in Figures 4a-4h because they are obtained by driving pedal, while those of Figures 4 are obtained by driving rudder directly. The rudder obtained from the pedal inputs matches the Figure 4a rudder very well, but not perfectly. Note that the pedal used matches the FDR recorded pedal rather well, though this was not an objective when selecting the pedal inputs; they were selected solely to give the desired rudder deflection.

The same pedal that was used to generate the “Simulator, with yaw damper override” curves was used to generate the “Simulator, without yaw damper override” curves. In the latter simulation, the yaw damper commands were allowed to contribute to the commanded rudder position, and the pedal rudder commands were constrained to the RTLU limits. Note that in the simulation, the RTLU limit is applied to the rudder command resulting from the pedal input, not to the pedal signal itself, which can exceed the limit. The sum of the rudder command from the pedal and the yaw damper is also limited by the RTLU.

In the bottom graph of Figure 6b,

Rudder (2) = Rudder from the simulation without yaw damper override (pedal limiter implementation)

Rudder (1) = Rudder from the simulation with yaw damper override (baseline A300)

Note that the difference between Rudder (2) and Rudder (1) is not identical to the yaw damper command, though it is similar. The additional difference is due to the fact that the final rudder position is not simply the sum of the rudder commands from the pedal and yaw damper, but includes the dynamics of the rudder servo, which depend on the difference between the commanded and actual rudder position. The servo dynamics are modeled in the simulator as a first order lag filter; the response of the filter therefore depends on time and the input signal, which is the error between the commanded and actual rudder position.

Figures 6c-6e show that the thrust, external moments, and winds used in the simulation are identical to those used in previous simulations.

Figure 6f compares the Euler angle response of the simulations with and without the pedal limiter system. The pitch response in both cases is similar, but the roll and yaw excursions, though still present, are somewhat diminished with the pedal limiter system. These results

are mirrored in Figure 6g, which shows the angle of attack and sideslip angle response. The angle of attack is almost identical for the two systems, but the maximum values of the sideslip angle excursions are reduced with the pedal limiter system.

Similar trends are seen in the load factor results plotted in Figure 6h. There is almost no difference between the two simulations for the longitudinal and normal load factors, but there is a noticeable difference in the lateral load factor. The altitude and airspeed response, shown in Figure 6i, is similar for the two systems.

4. CONCLUSIONS

4.1. Data Latency

The results discussed in Section 3.1 indicate that for dynamic maneuvers involving high angular rates, the time delays in the Euler angles can introduce significant error into the time relationships between parameters recorded on the FDR. These errors propagate to parameters derived from the recorded data, such as sideslip angle and loads. Correcting for the estimated effect of these latencies in the AAL587 data shifts the calculated sideslip forward in time by about 0.25 seconds, so that at the time of tail separation the sideslip angle is about 2° higher than that computed previously. The uncertainty in the sideslip angle calculation and resulting tail loads associated with various combinations of the full range of possible data latency values is still under investigation.

In general, during accident investigations a proper synchronization of all data recorded on the FDR and derived from data recorded on FDR is fundamental. Data latencies introduce uncertainties into these synchronizations that can only be accounted for approximately, since the latency values are not known precisely and can vary, within certain ranges, from sample to sample and parameter to parameter. The significance of these uncertainties and the degree to which they hamper a proper analysis of the data depends on the sensitivity of the analysis to small changes in the data, and the dynamic nature of the maneuver being analyzed.

4.2. NTSB Simulations

The simulator match of the accident maneuver discussed in Section 3.2.1 indicates that while external winds and moments, assumed to be attributable to the wake encounter, are required to match the motion recorded on the FDR, the large roll and yaw oscillations, lateral load factors, and sideslip angles achieved during the maneuver are the result of wheel and rudder inputs. By themselves, the external winds and moments only produce an initial 10° deviation in bank angle and only subtle changes in heading, resulting in sideslip angles of less than 2.5°.

The difference between the simulator sideslip angle and the sideslip angle computed from the FDR data shows the significant effect low sampling rates of key parameters such as the Euler angles can have on the results of calculations using these parameters. In the present case, differences of 1° of sideslip are important when considering loads on the vertical tail. Other difficulties caused by low sample rates, including computing load factors in the cockpit and determining cockpit control and control surface positions, are discussed in Section D-IV of the *Aircraft Performance Study*.

The simulation of the accident maneuver with a pedal limiter system, discussed in Section 3.2.2, indicates that such a system prevents the pilot from overriding yaw damper inputs at the rudder limits, and allows the yaw damper to attenuate (but not prevent) the development of the sideslip angle.

5. REFERENCES

1. Airbus Industrie Document #506.0009/2001, Edition 04, "AAL587 Accident (A300-600 MSN 420) at New York on 12 Nov. 2001 - Time Delays for Recorded Parameters," issued June 15, 2003.

6. CORRECTION

The altitude labels in Figure 8 of the *Aircraft Performance Study* contain errors. The corrected Figure is presented here as Figure 7.

John O'Callaghan
National Resource Specialist - Aircraft Performance

FIGURES

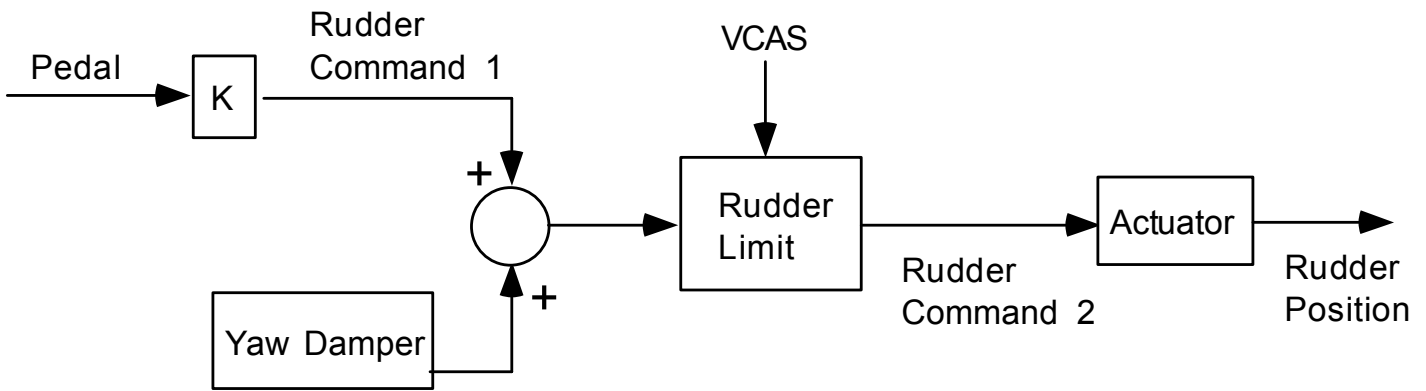
Actual system

Figure 1a. A300 rudder control system schematic.

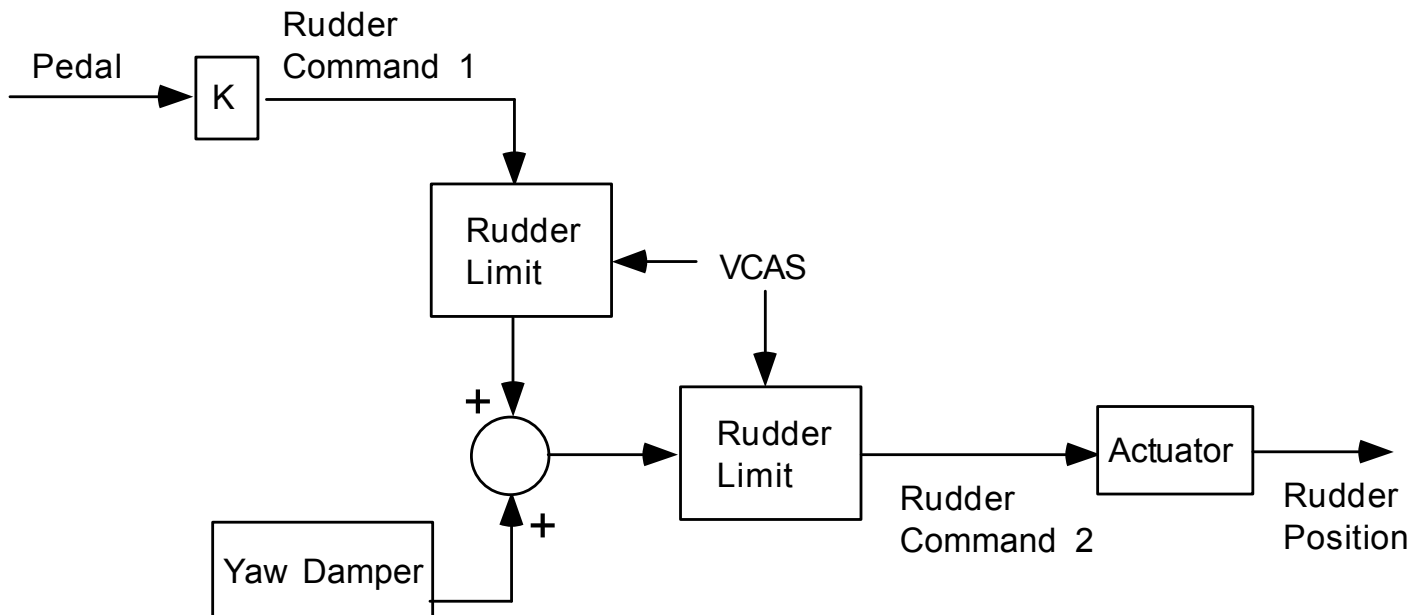
System with pedal limiter

Figure 1b. Rudder control system with pedal limiter.

Euler Angles Adjusted for Time Latency

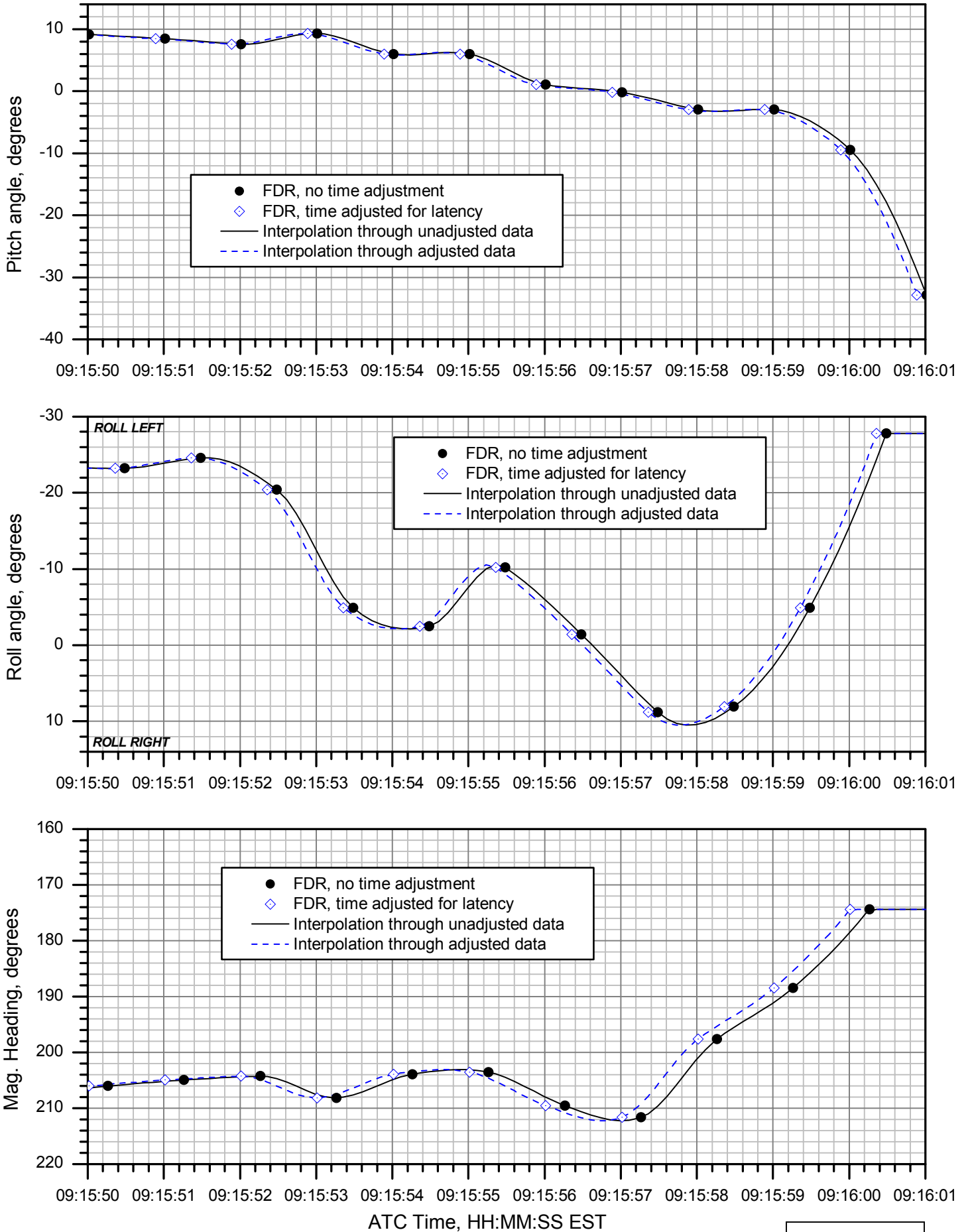


Figure 2.

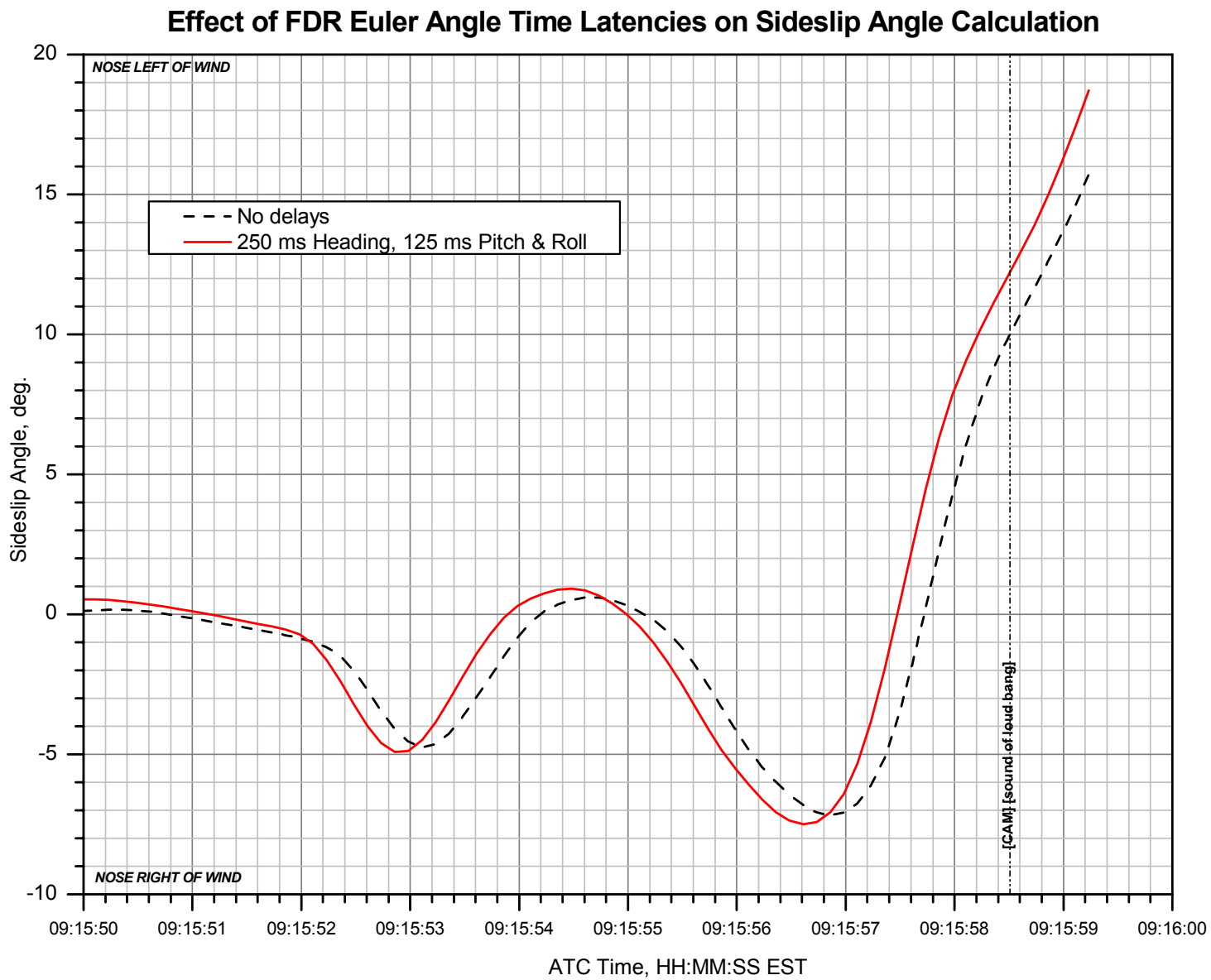


Figure 3.

AAL587 Simulator Match: Controls

NTSB Match v17

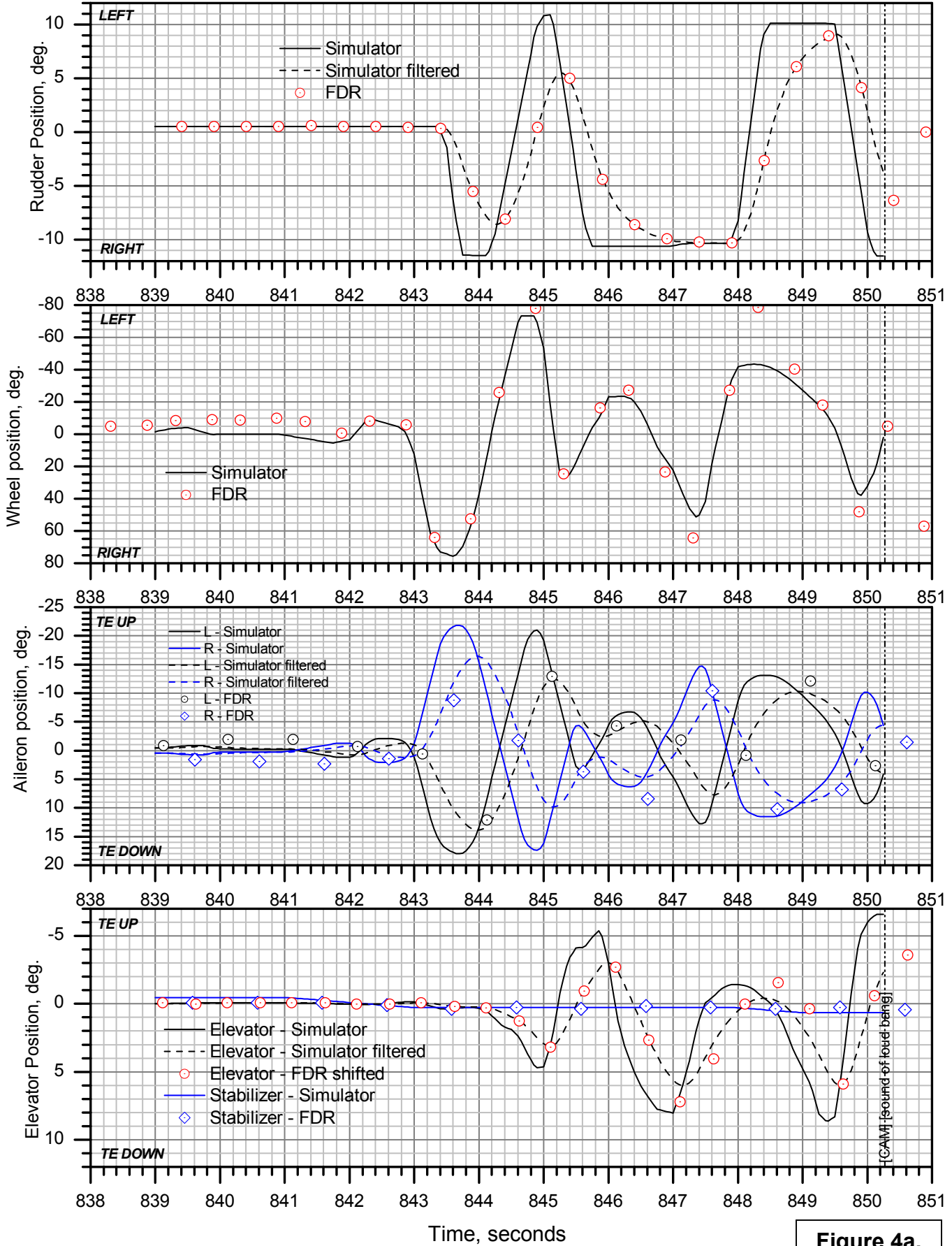


Figure 4a.

AAL587 Simulator Match: Thrust

NTSB Match v17

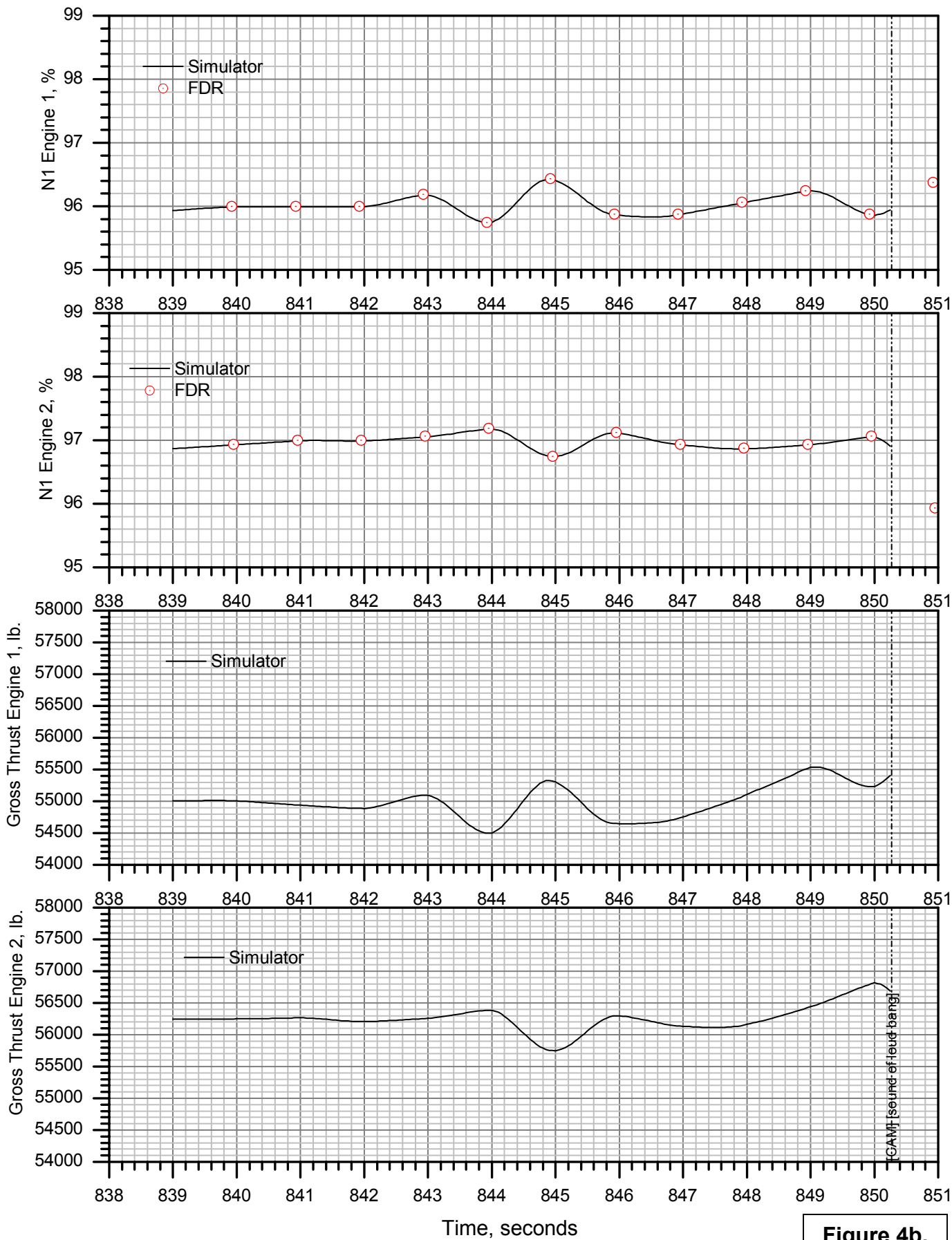


Figure 4b.

AAL587 Simulator Match: External Moments

NTSB Match v17

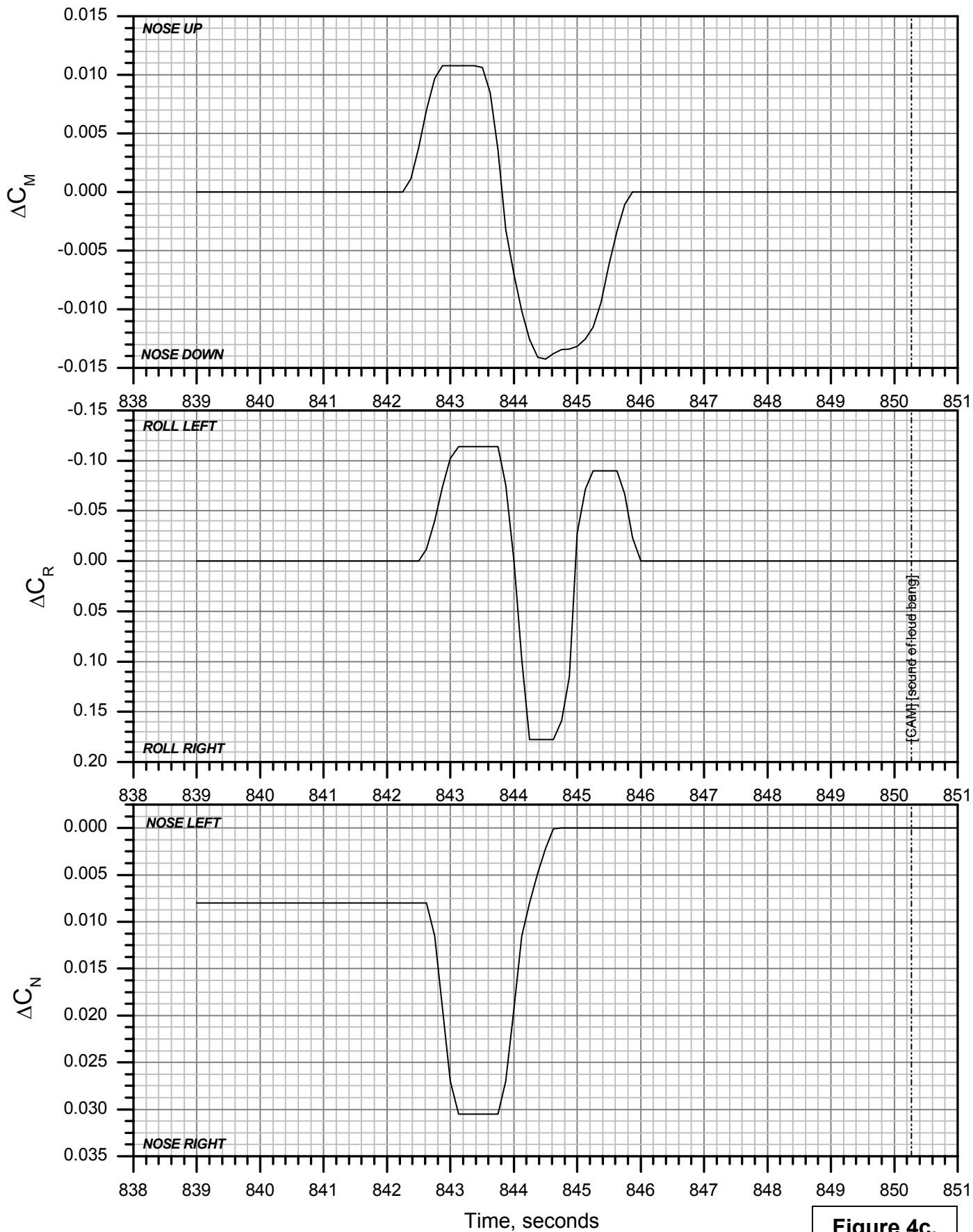


Figure 4c.

AAL587 Simulator Match: Winds

NTSB Match v17

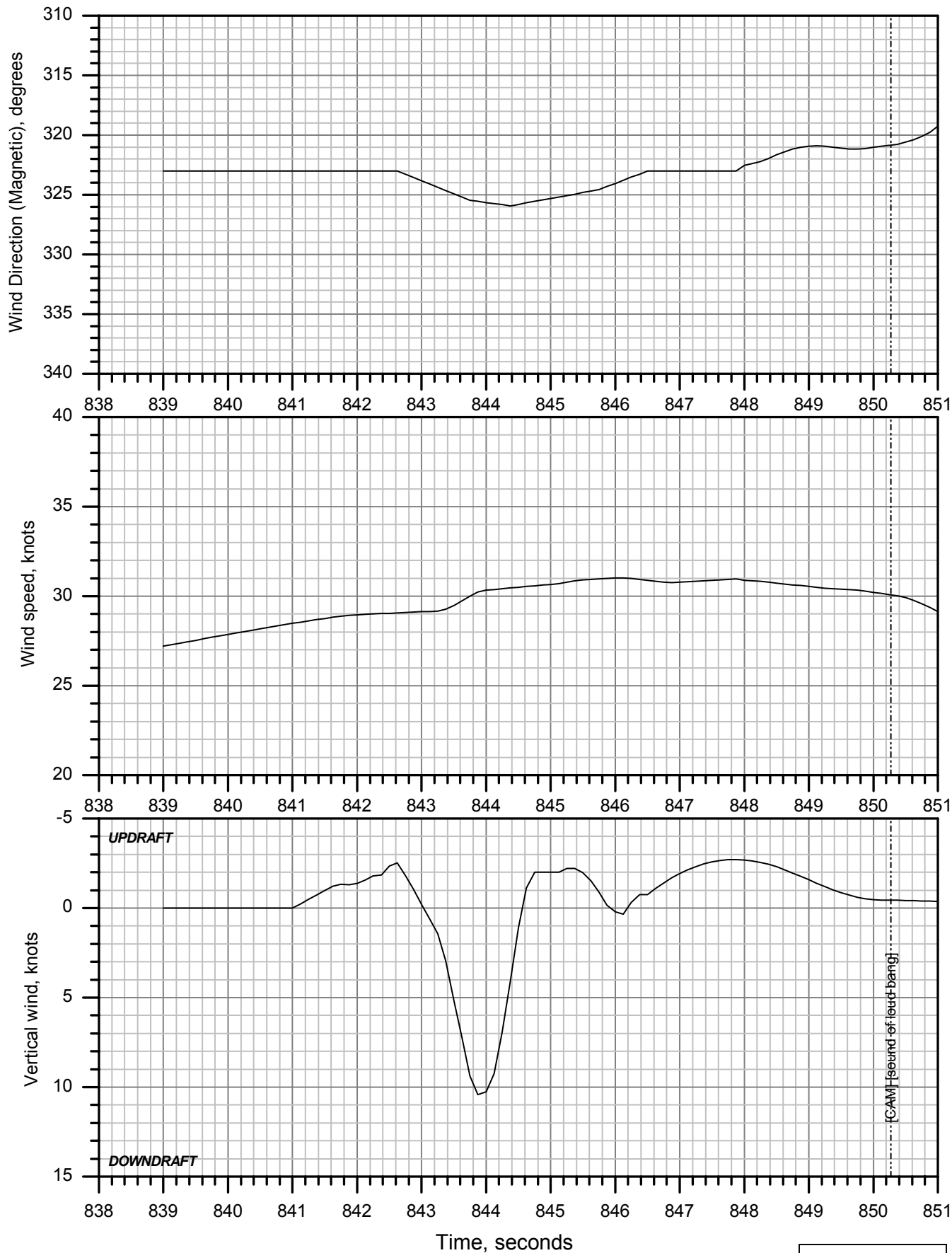


Figure 4d.

AAL587 Simulator Match: Euler Angles

NTSB Match v17

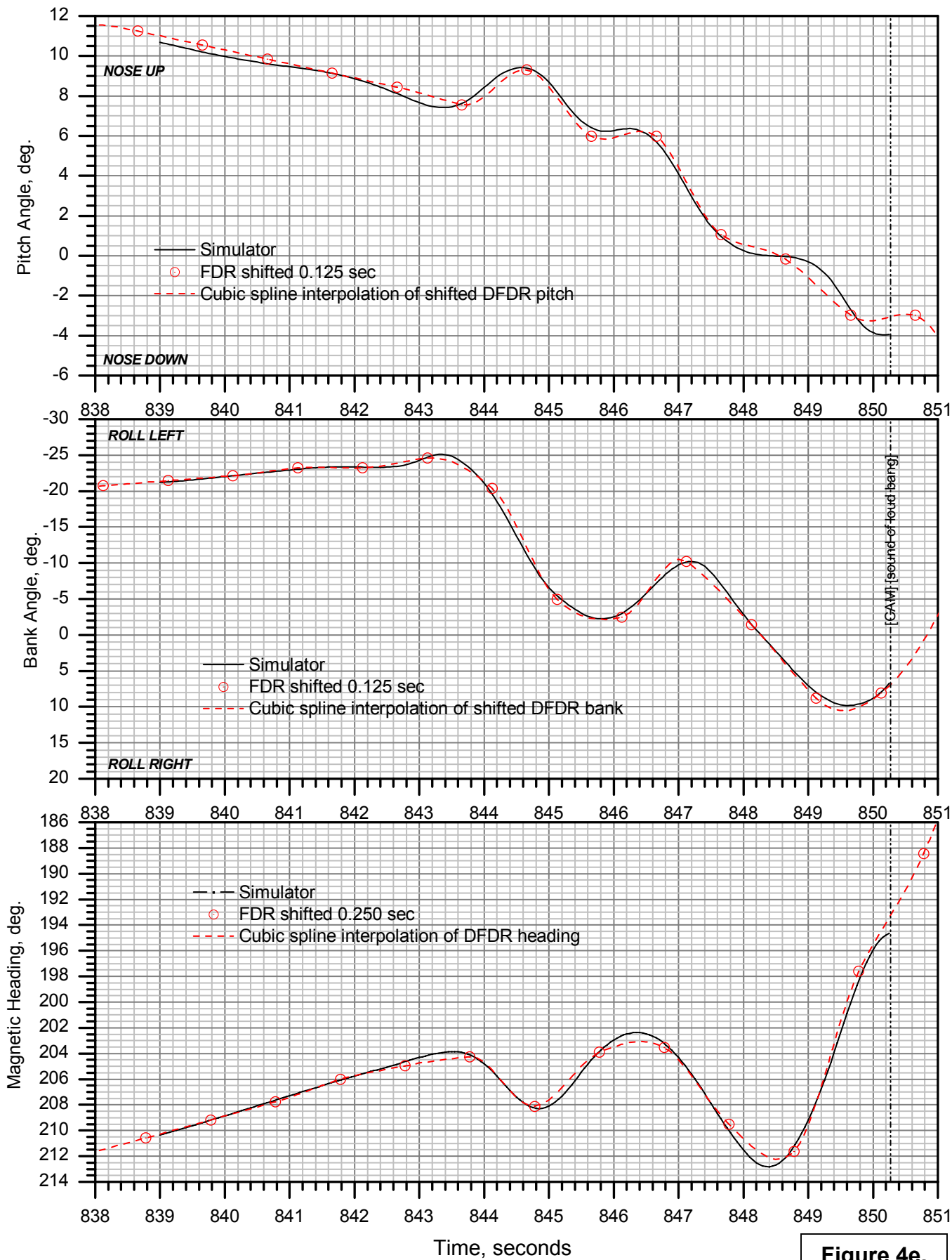


Figure 4e.

AAL587 Simulator Match: Angle of Attack & Sideslip

NTSB Match v17

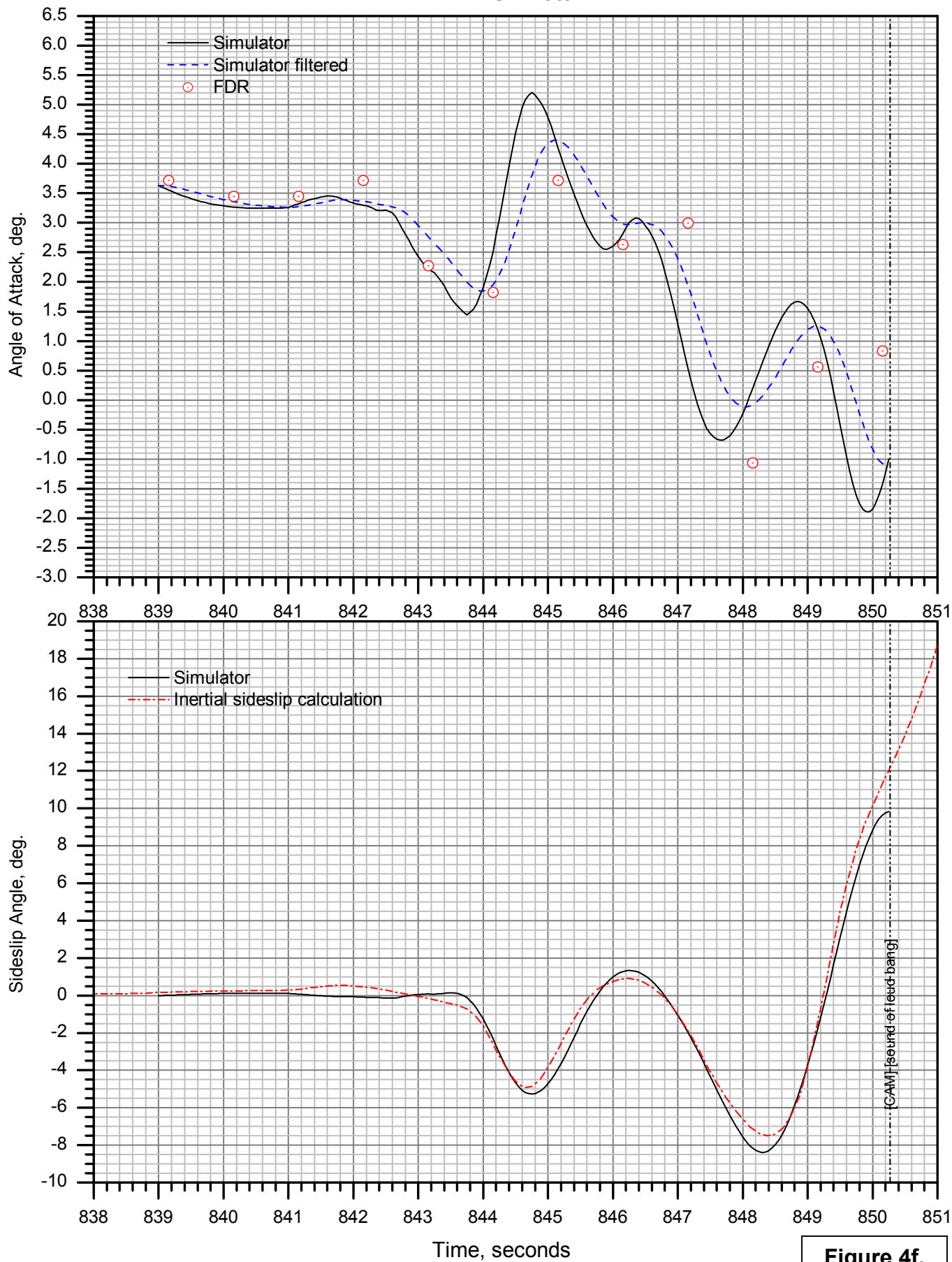


Figure 4f.

AAL587 Simulator Match: Load Factors

NTSB Match v17

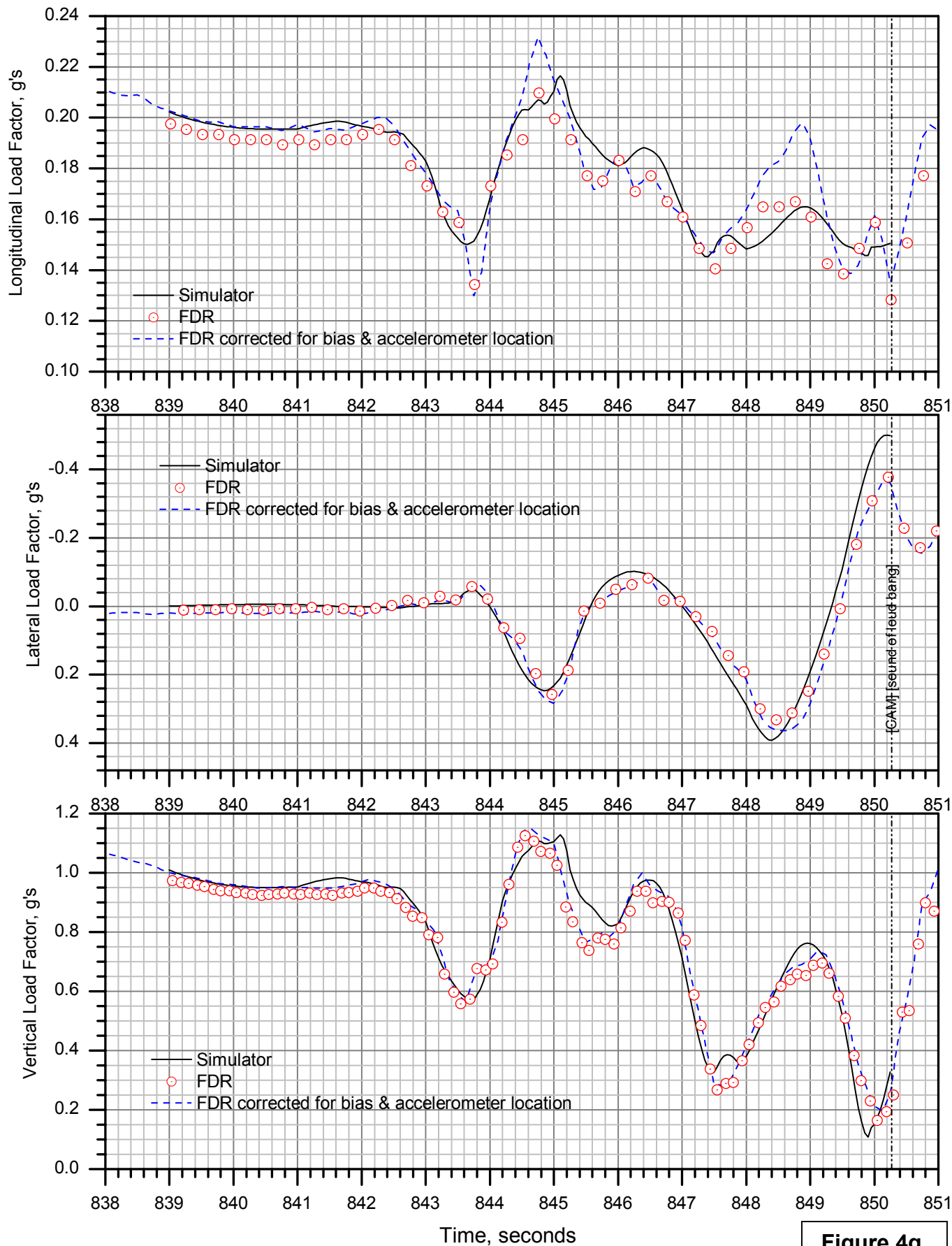


Figure 4g.

AAL587 Simulator Match: Altitude & Speed

NTSB Match v17

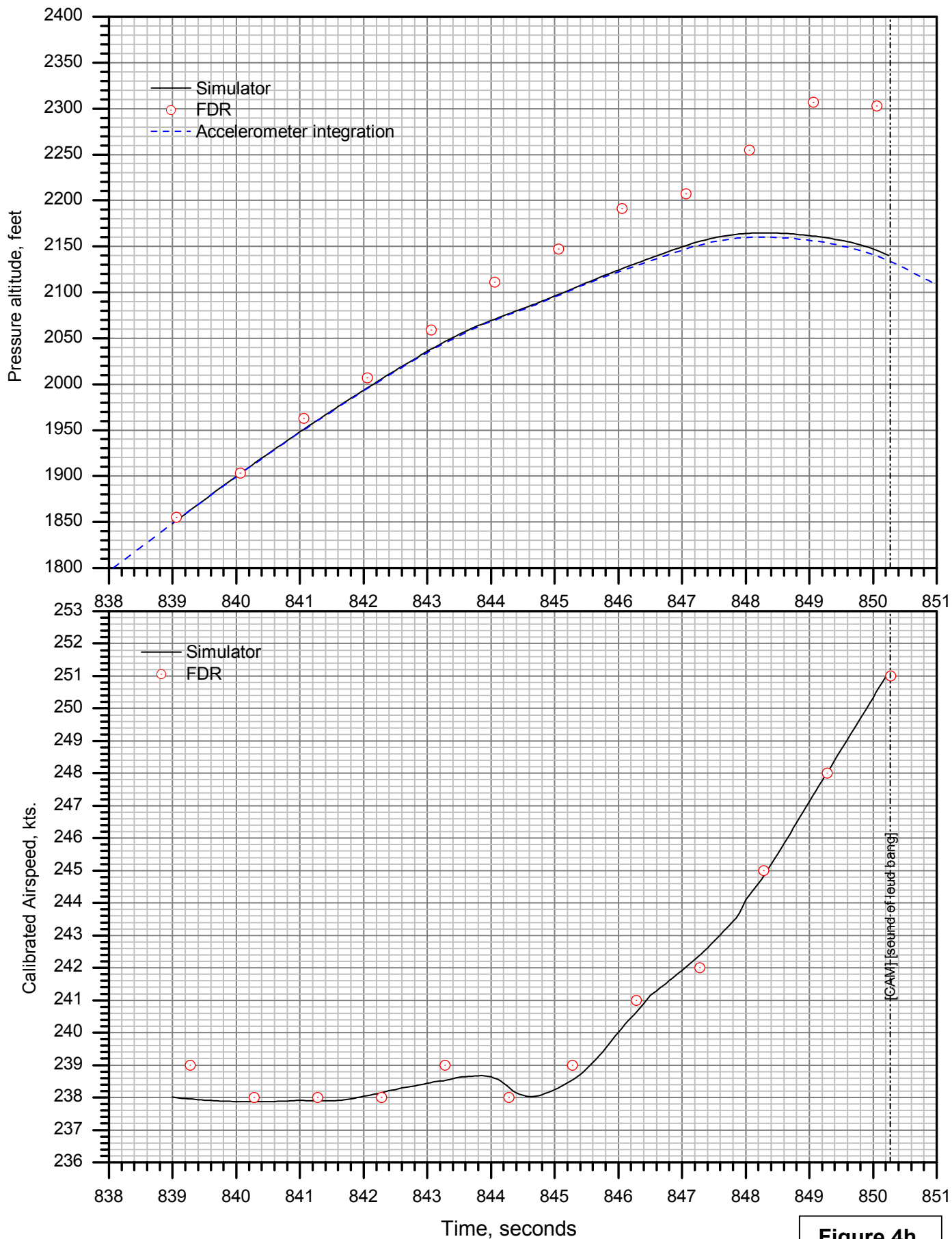


Figure 4h.

AAL587 Simulator Match: Controls

Vortex Effects with No Control Inputs

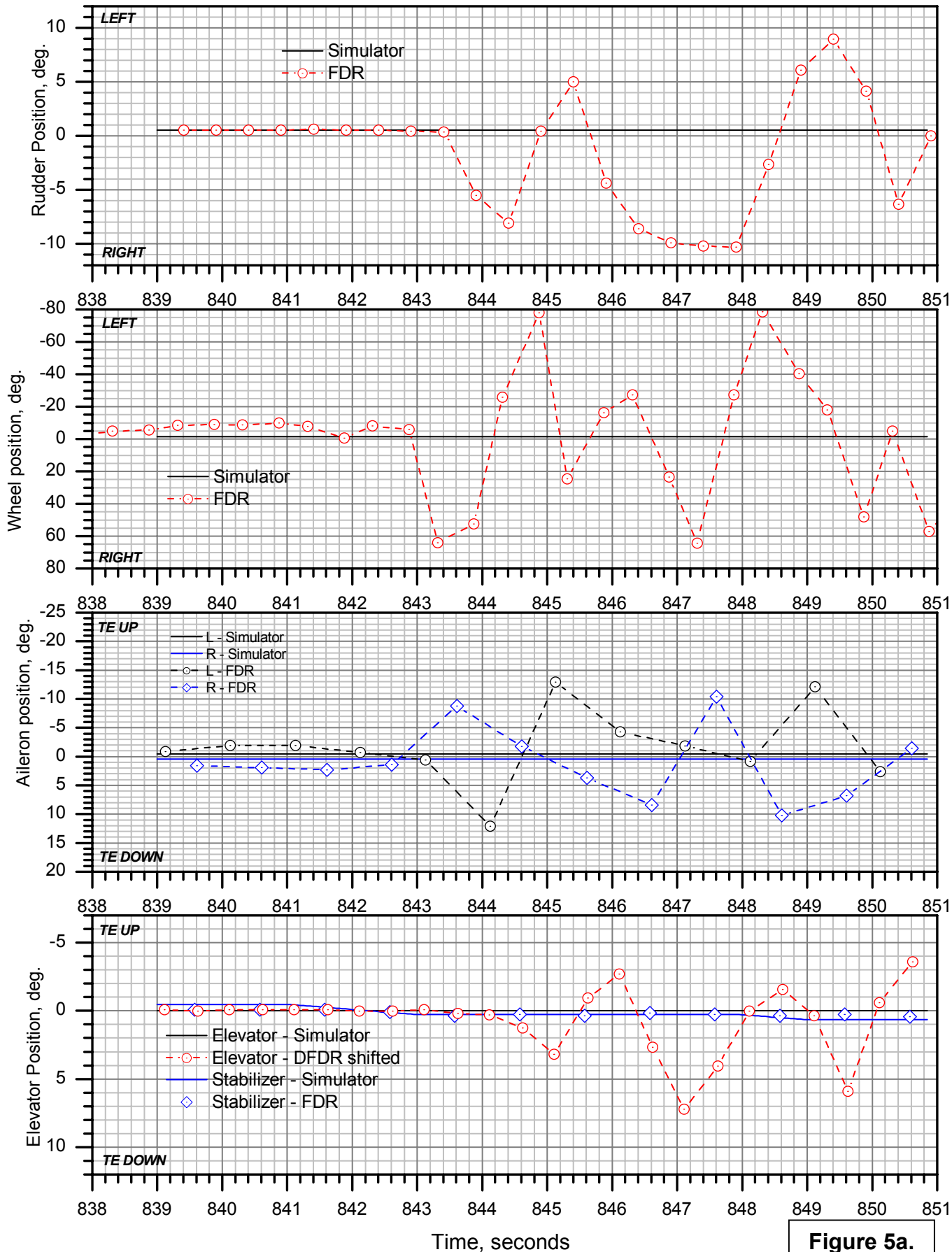


Figure 5a.

AAL587 Simulator Match: Thrust

Vortex Effects with No Control Inputs

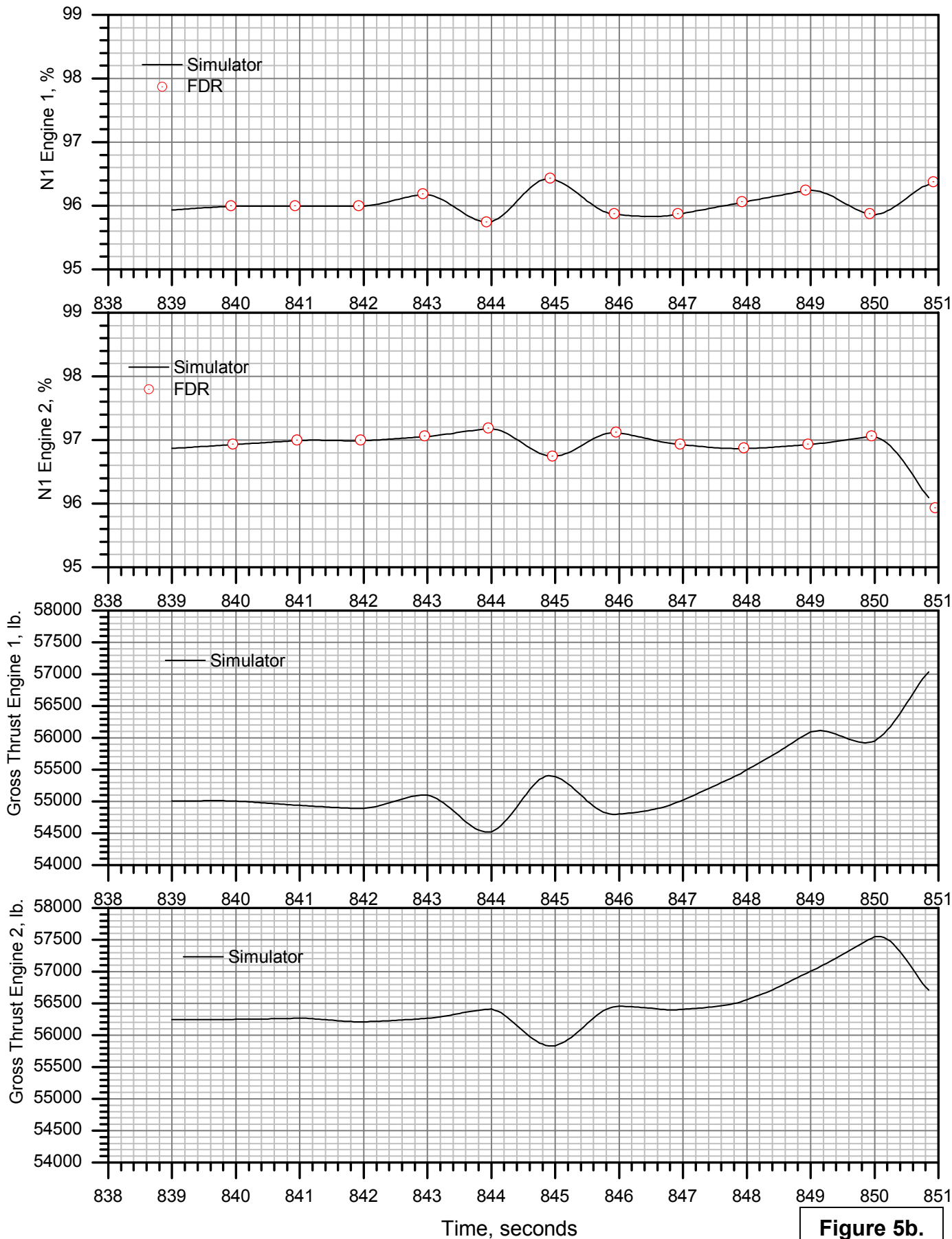


Figure 5b.

AAL587 Simulator Match: External Moments

Vortex Effects with No Control Inputs

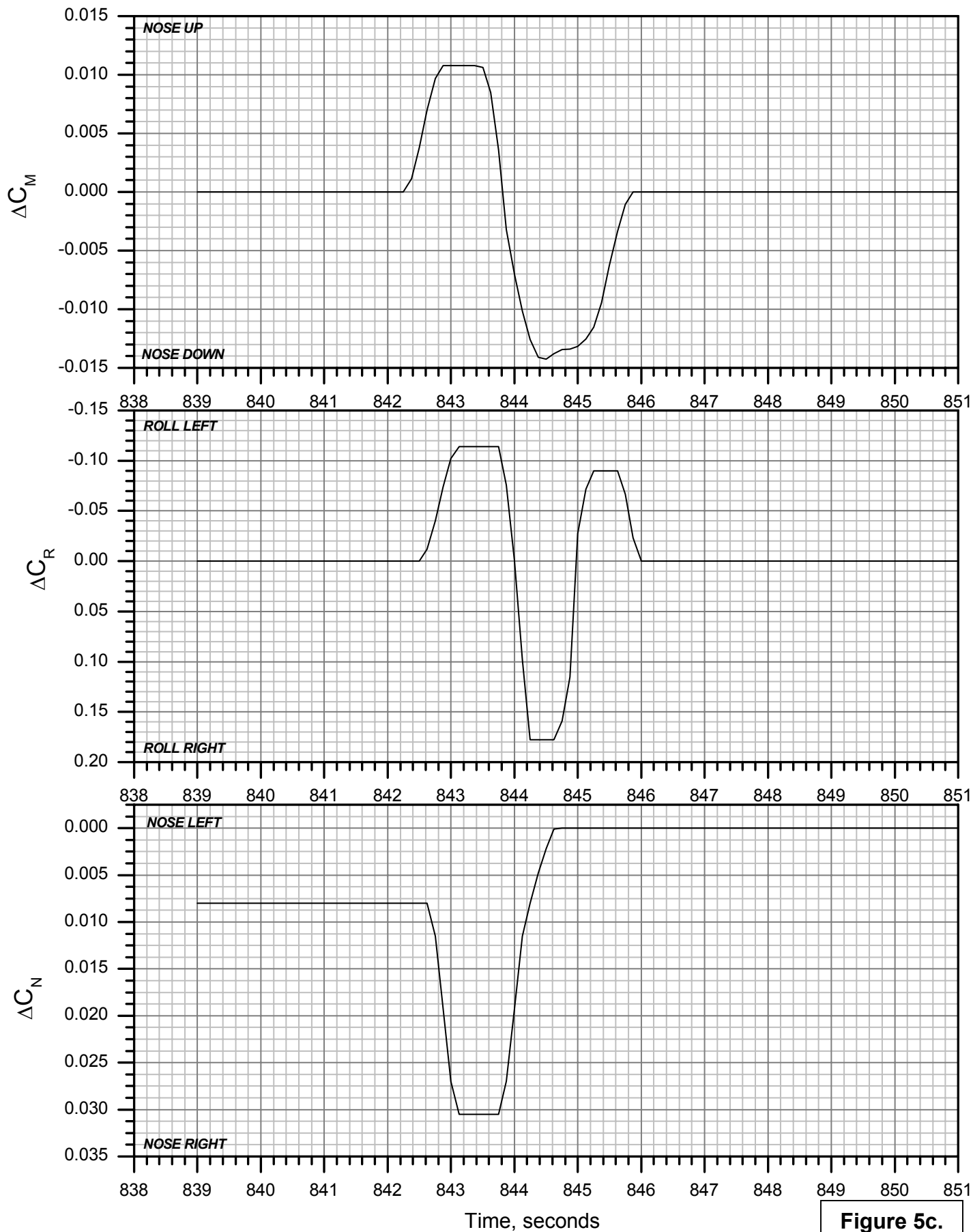


Figure 5c.

AAL587 Simulator Match: Winds

Vortex Effects with No Control Inputs

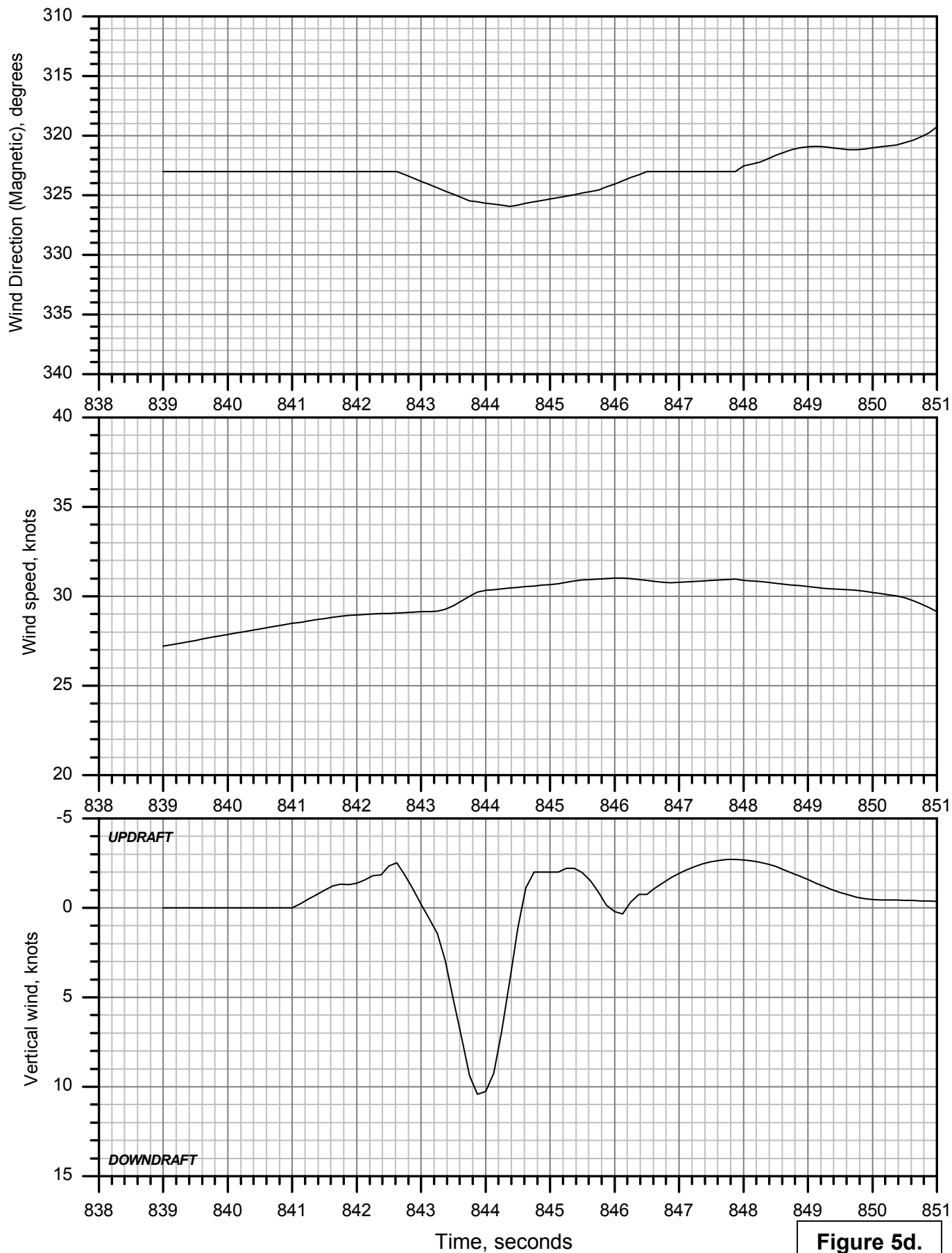


Figure 5d.

AAL587 Simulator Match: Euler Angles

Vortex Effects with No Control Inputs

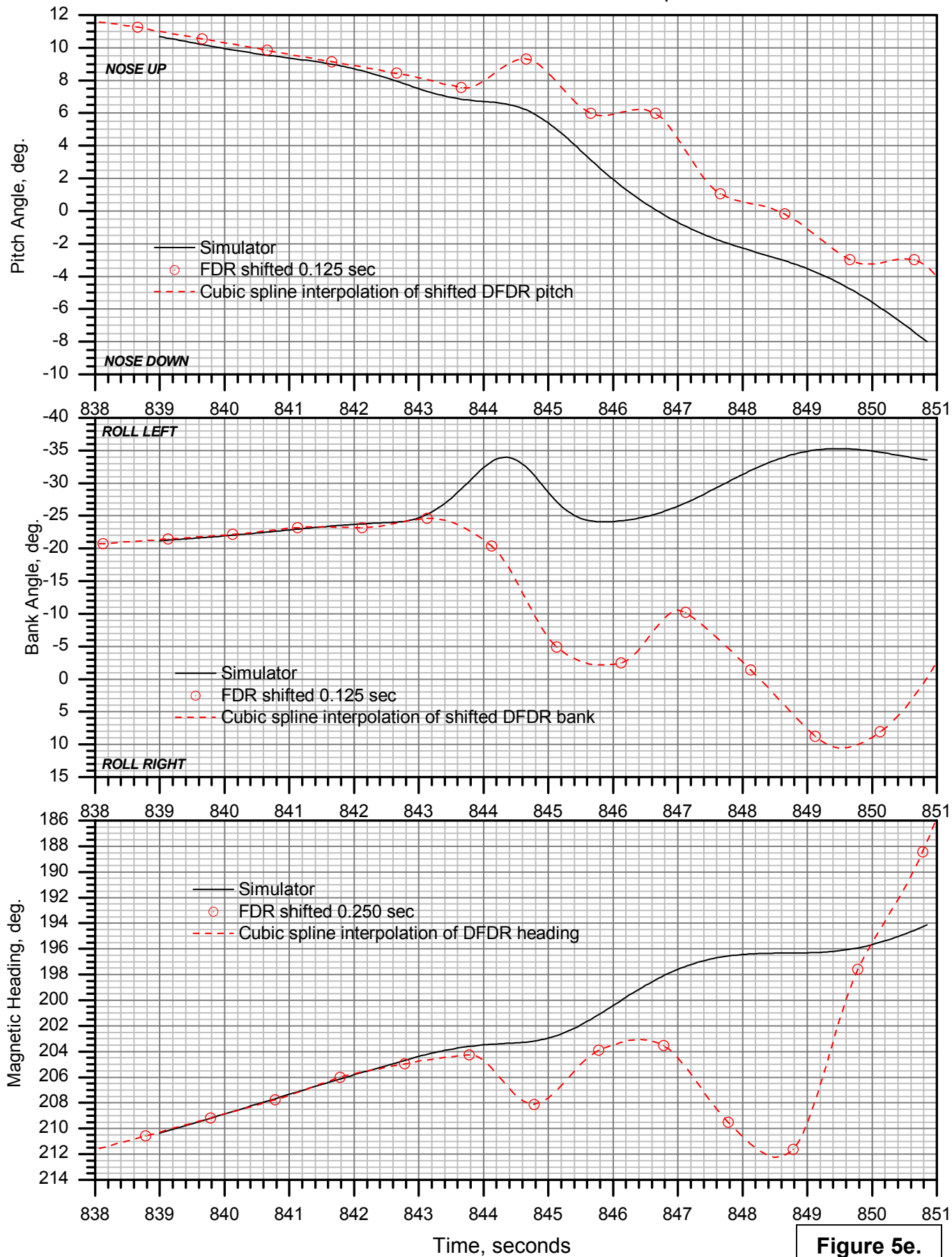


Figure 5e.

AAL587 Simulator Match: Angle of Attack & Sideslip

Vortex Effects with No Control Inputs

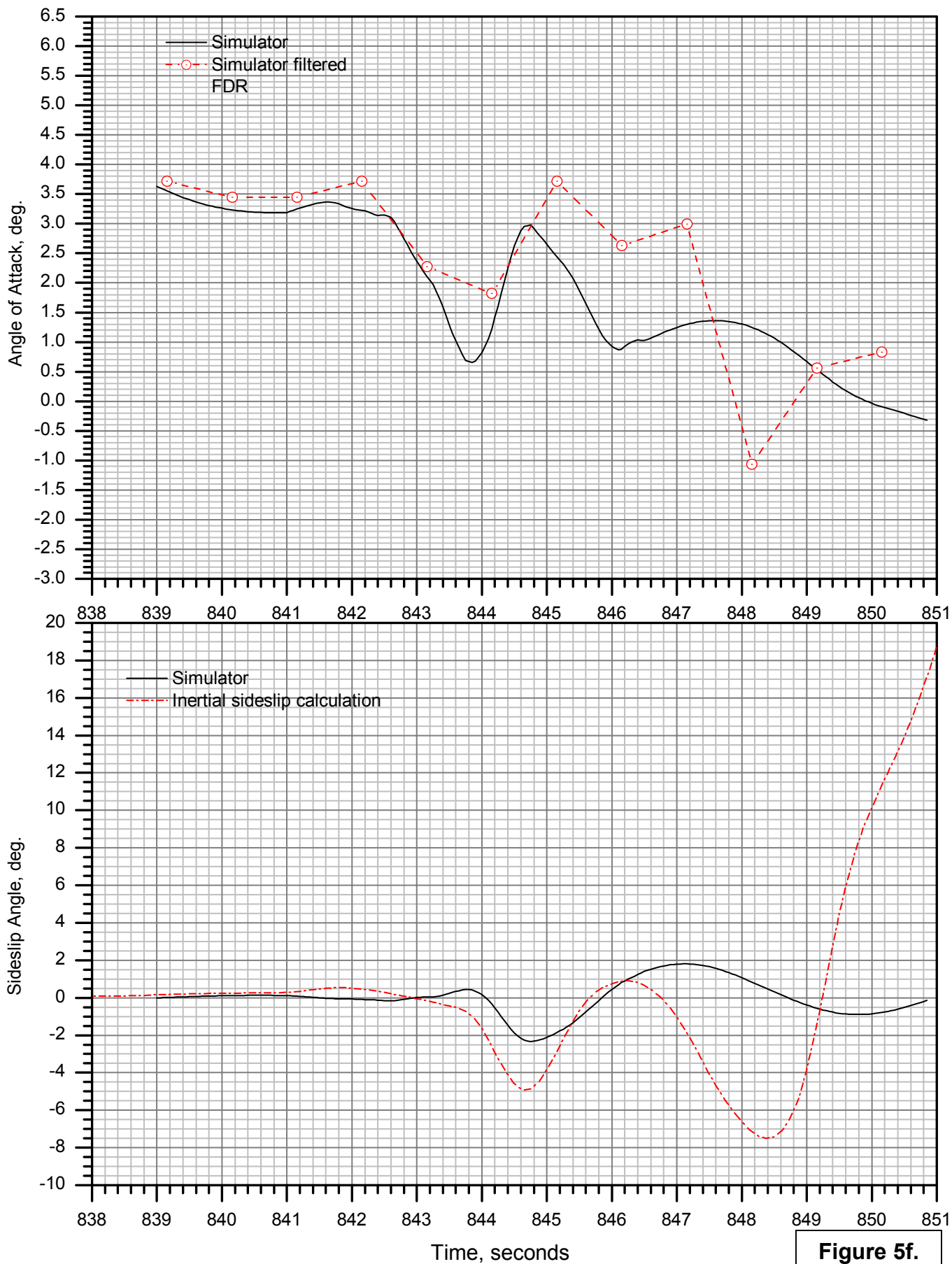


Figure 5f.

AAL587 Simulator Match: Load Factors

Vortex Effects with No Control Inputs

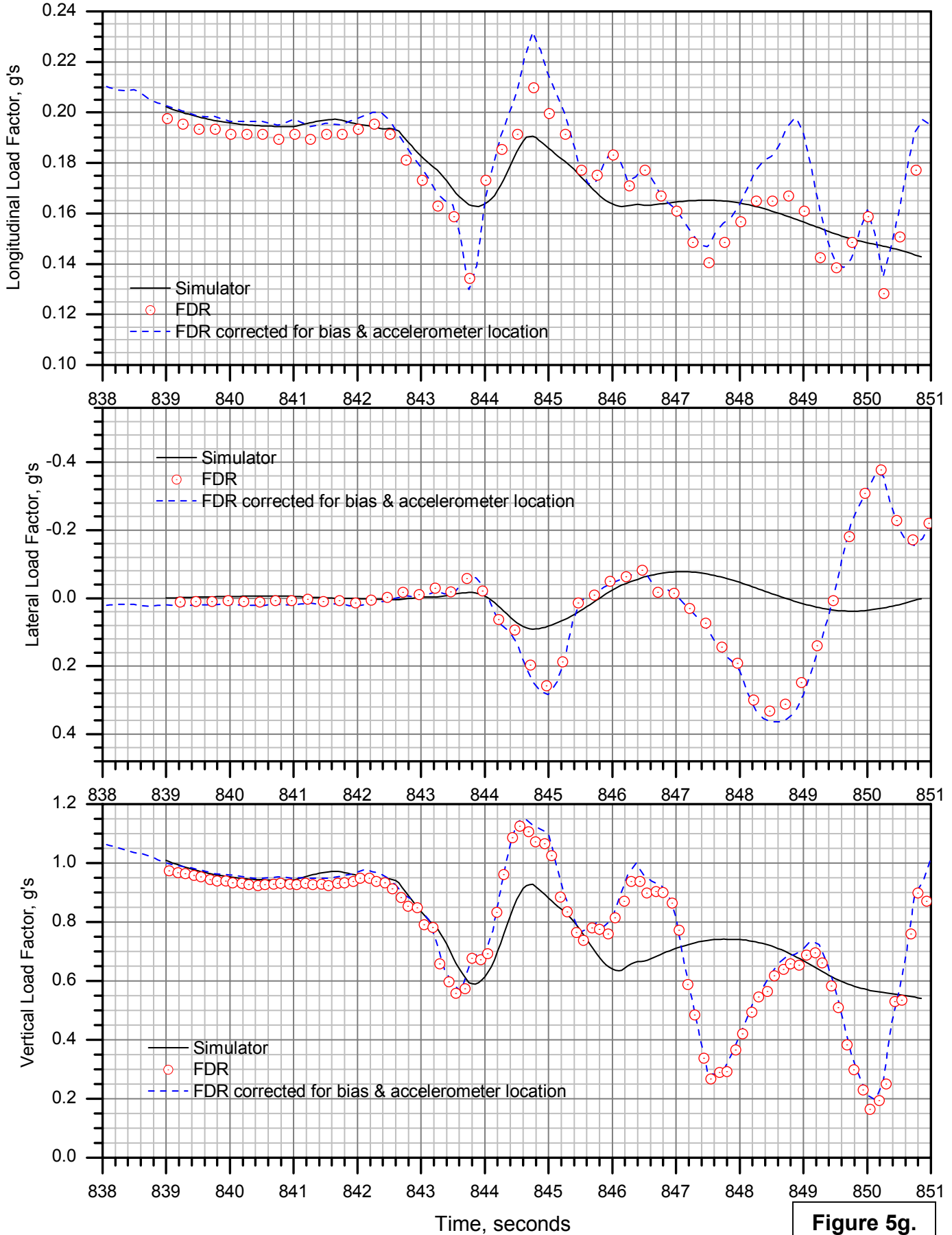


Figure 5g.

AAL587 Simulator Match: Altitude & Speed

Vortex Effects with No Control Inputs

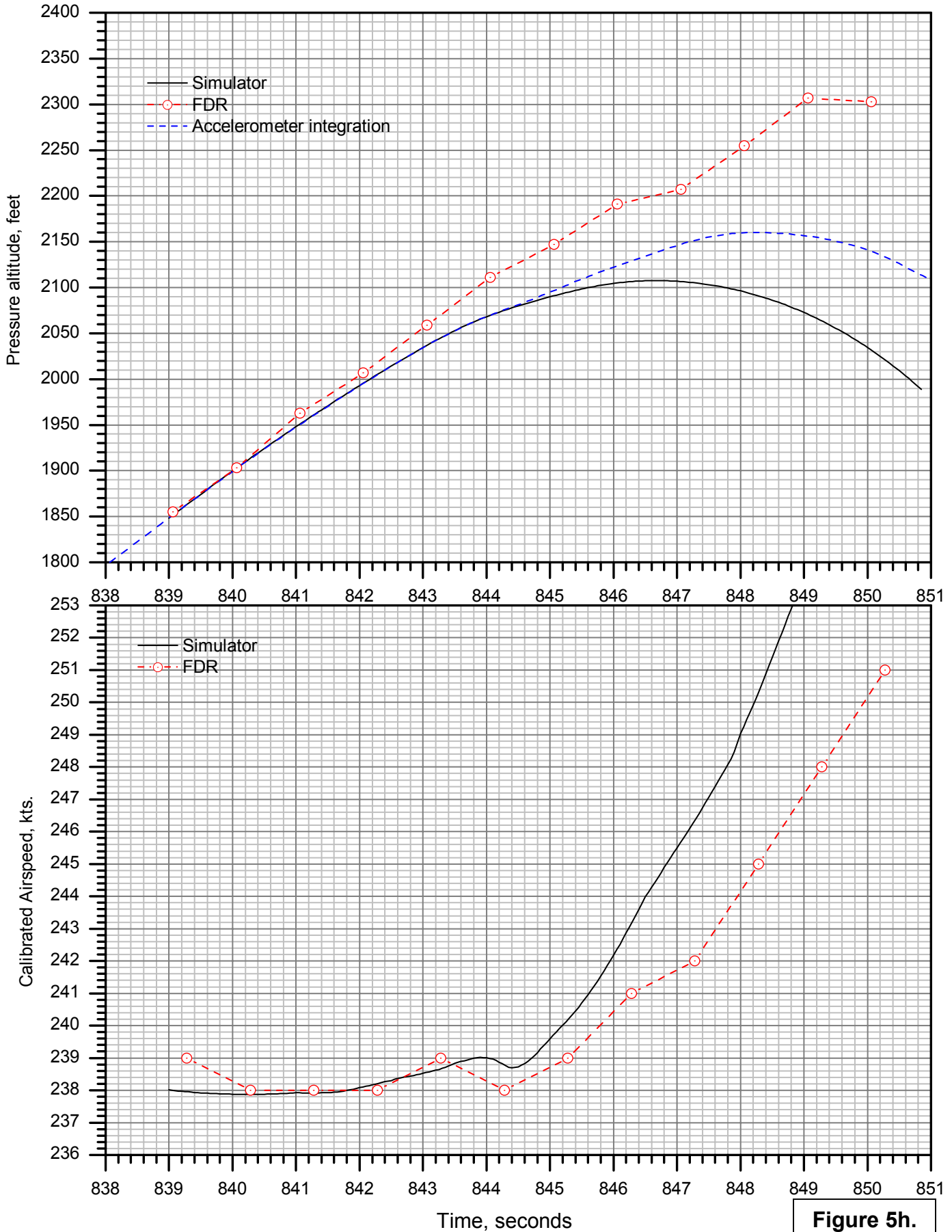


Figure 5h.

AAL587 Simulator Match: Controls

Yaw Damper Implementation Comparison

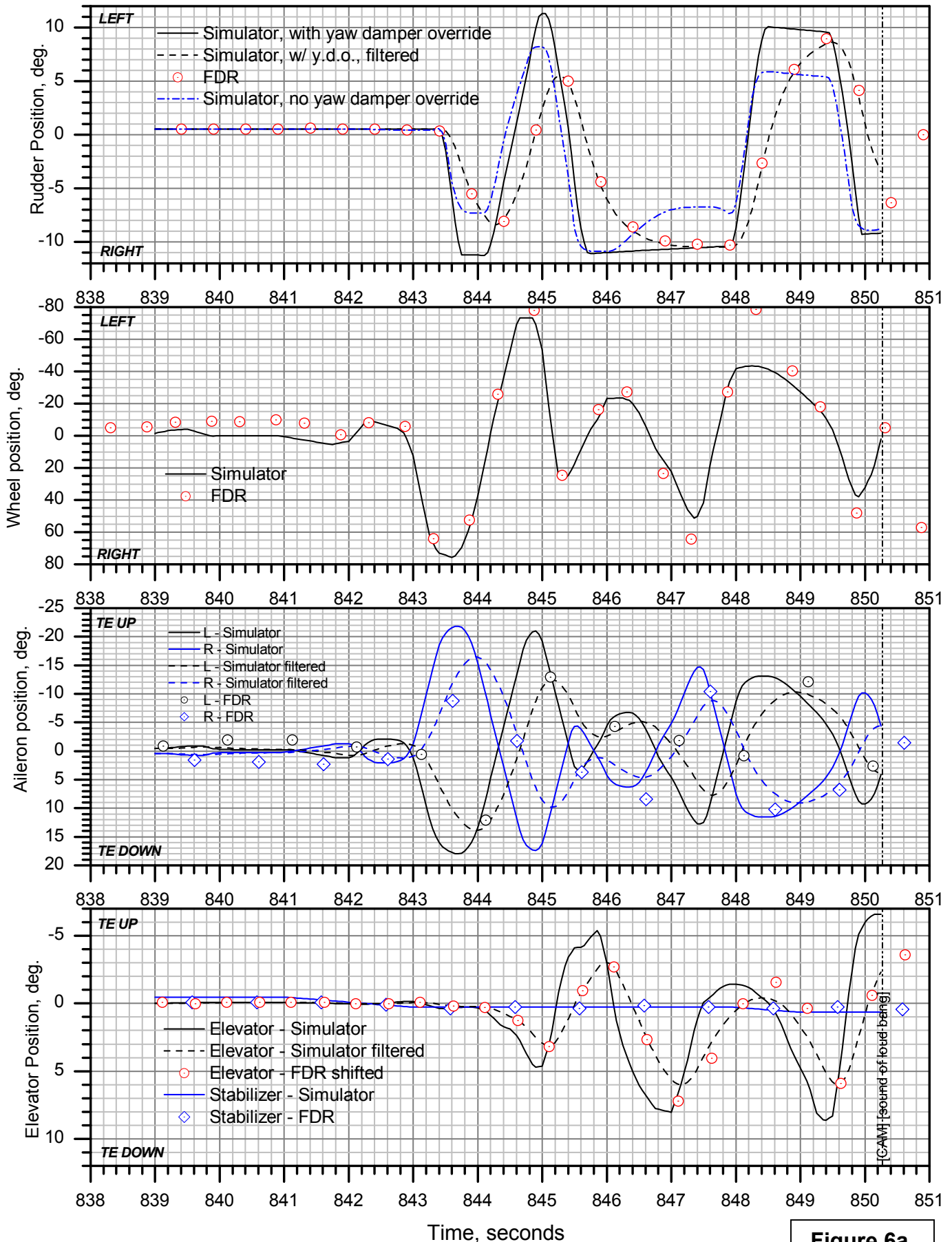


Figure 6a.

AAL587 Simulator Match: Pedal & Yaw Damper

Yaw Damper Implementation Comparison

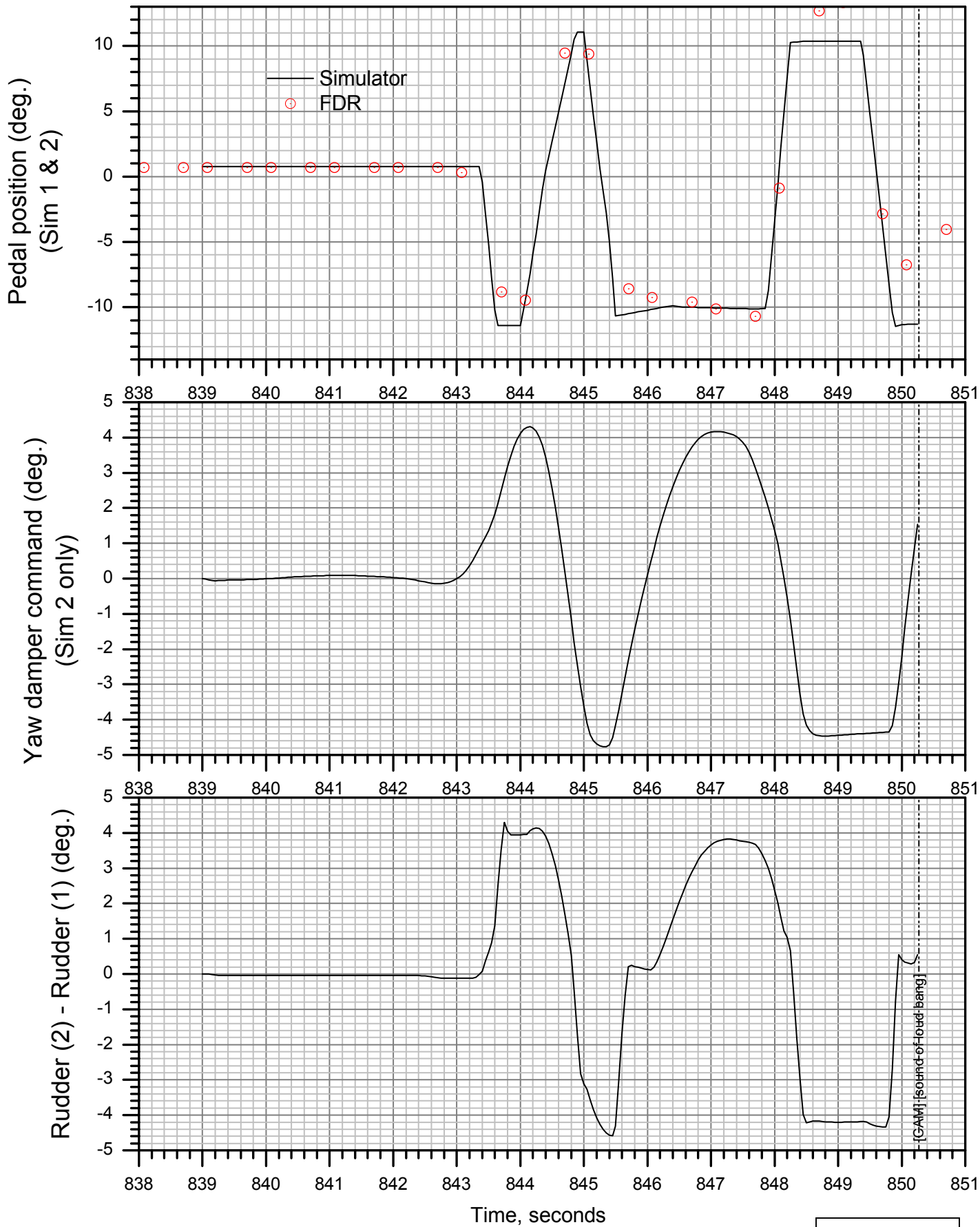


Figure 6b.

AAL587 Simulator Match: Thrust

Yaw Damper Implementation Comparison

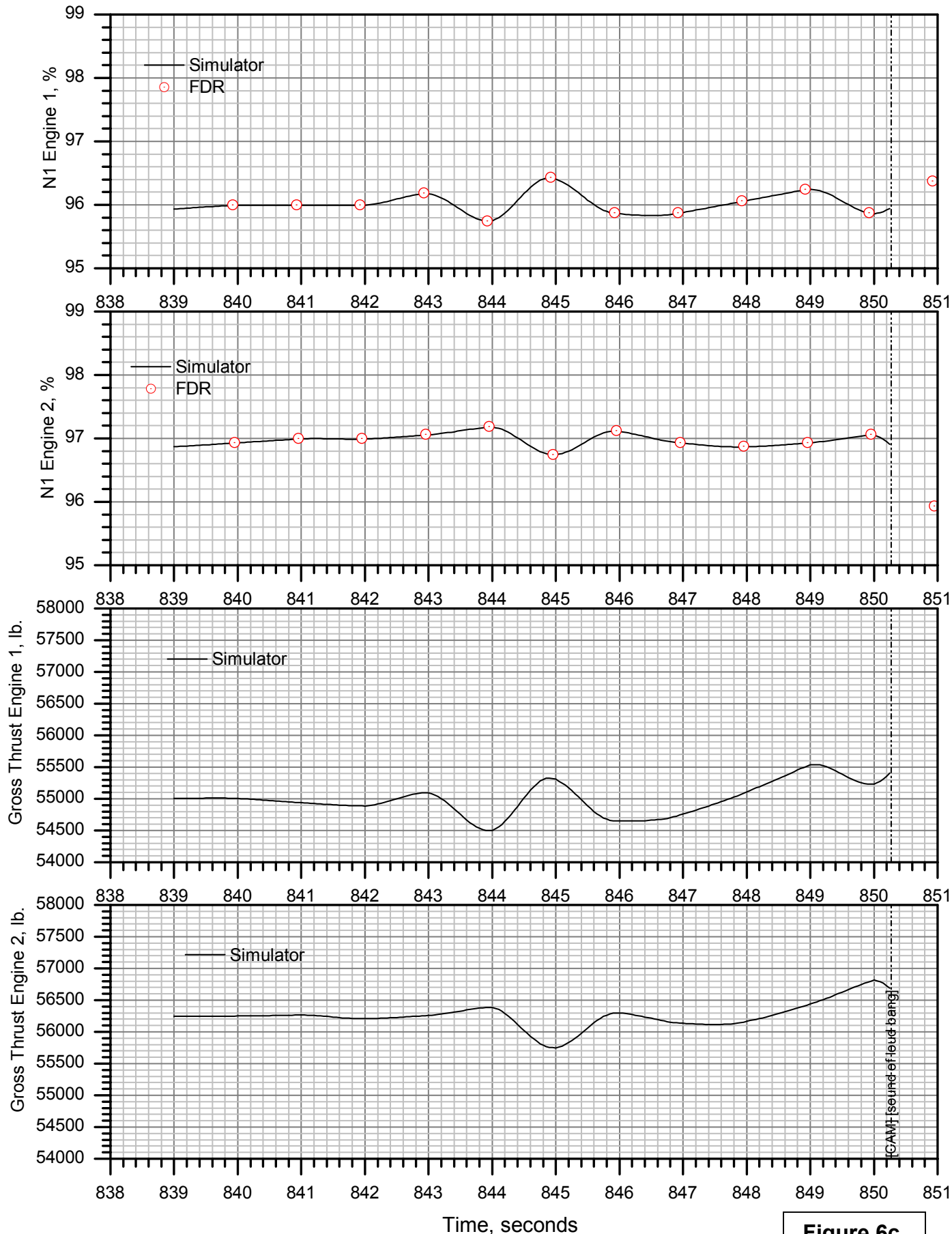


Figure 6c.

AAL587 Simulator Match: External Moments

Yaw Damper Implementation Comparison

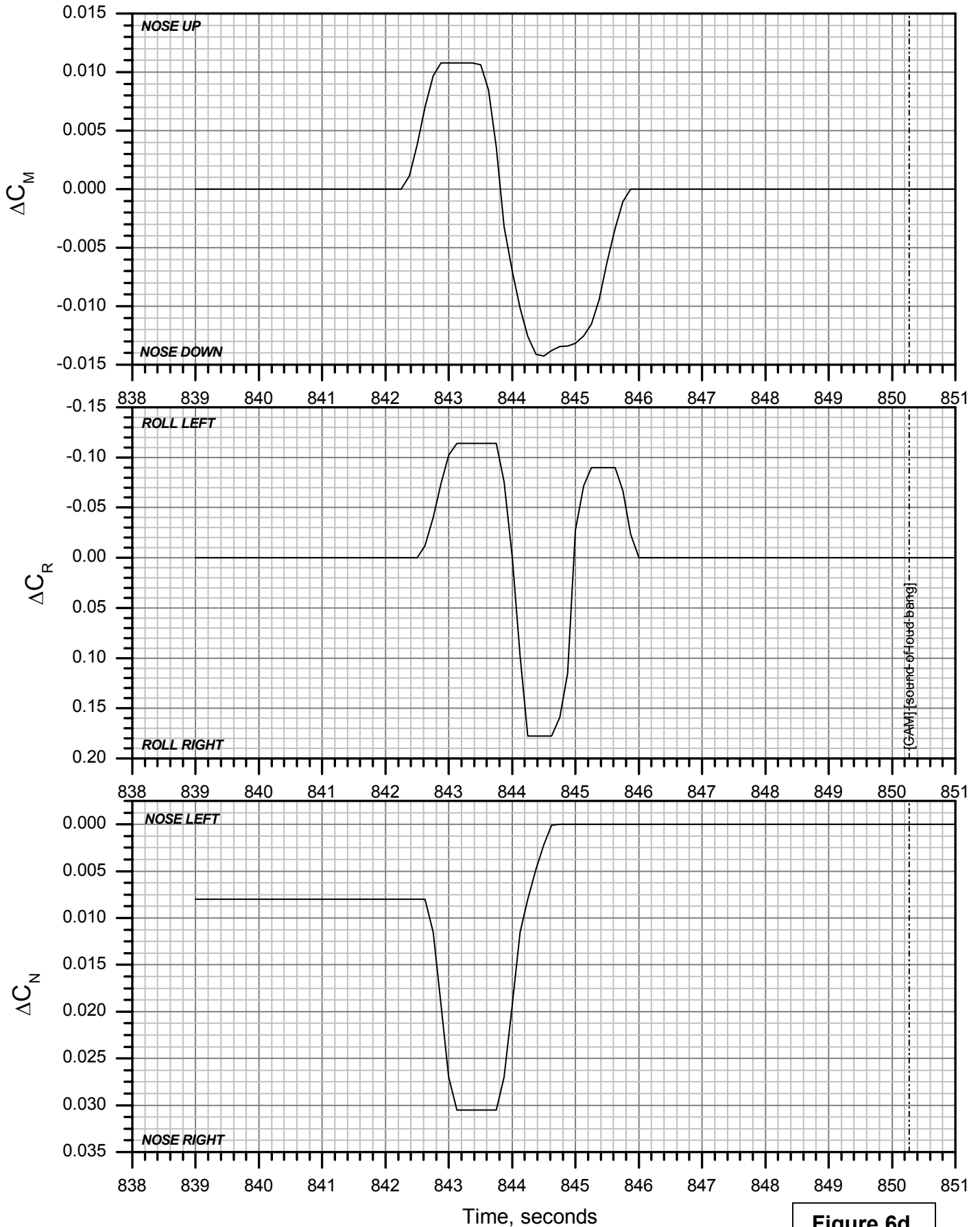


Figure 6d.

AAL587 Simulator Match: Winds

Yaw Damper Implementation Comparison

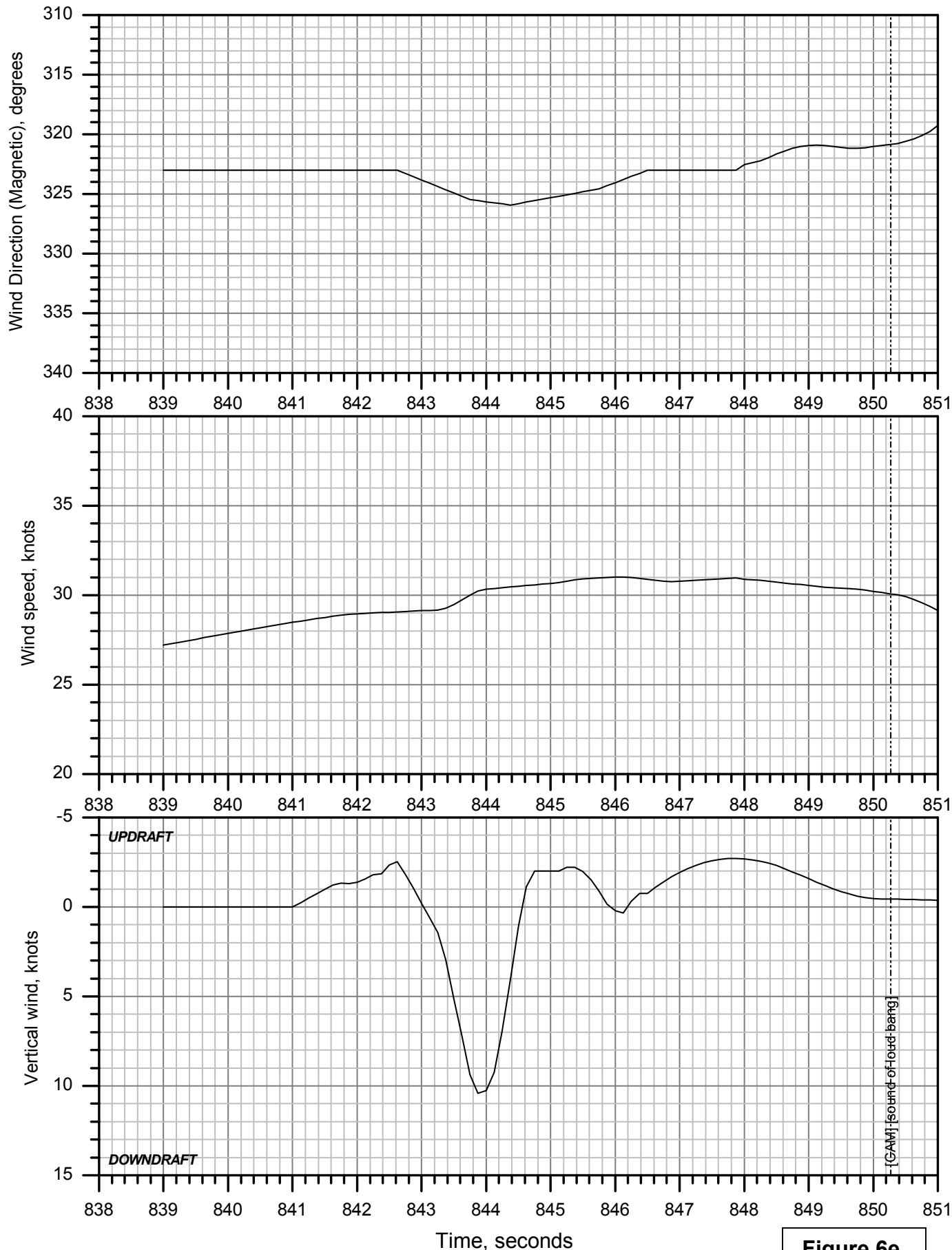


Figure 6e.

AAL587 Simulator Match: Euler Angles

Yaw Damper Implementation Comparison

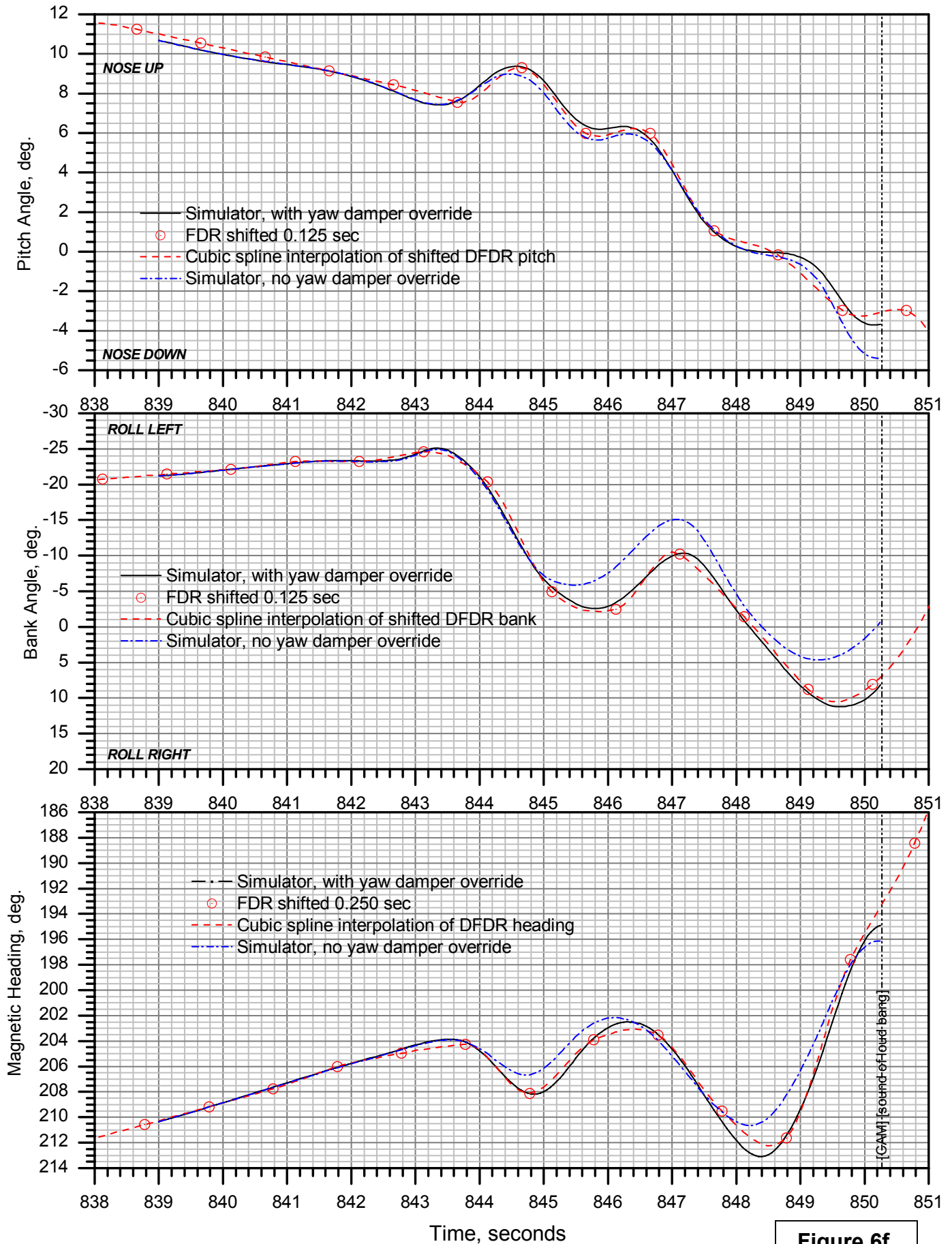


Figure 6f.

AAL587 Simulator Match: Angle of Attack & Sideslip

Yaw Damper Implementation Comparison

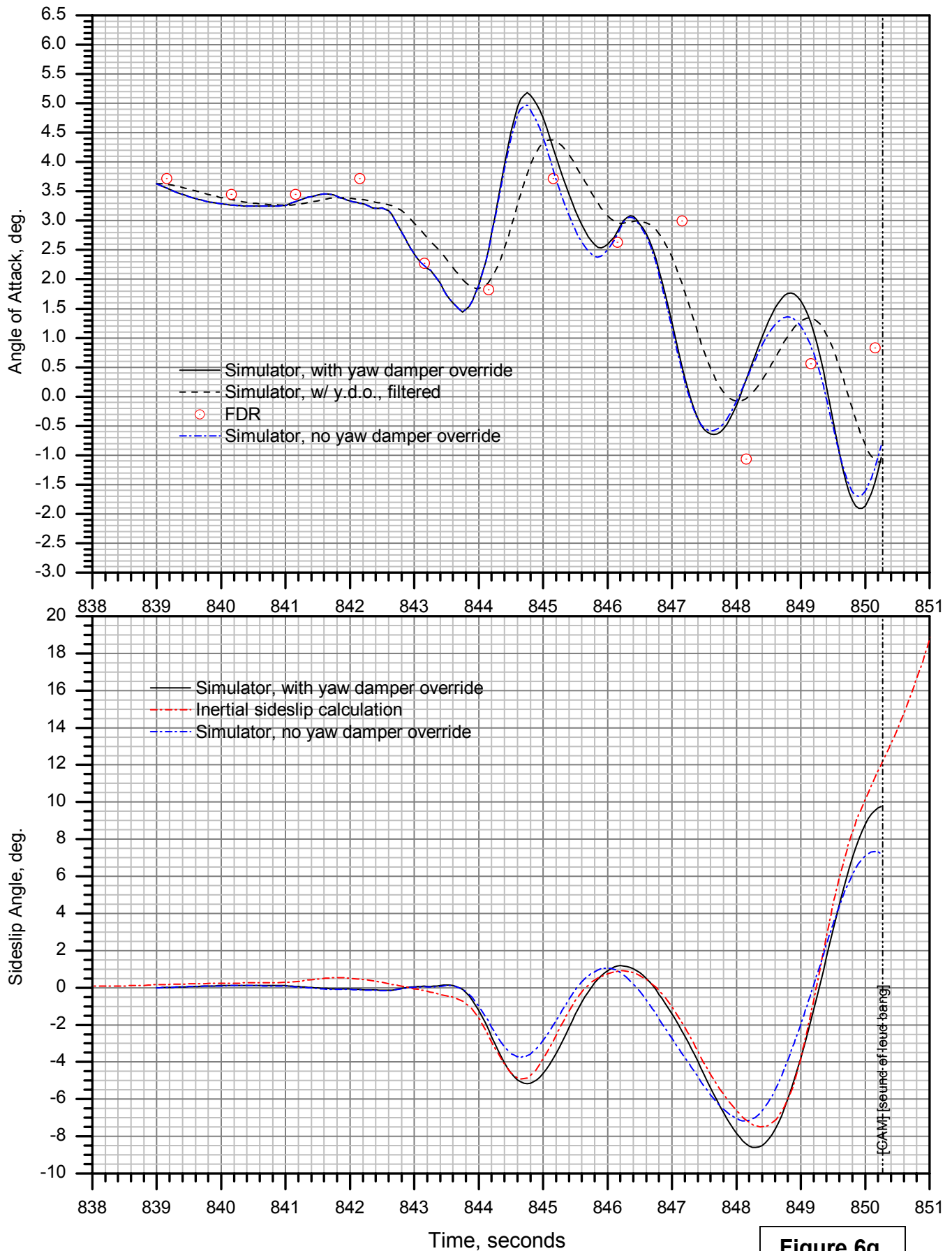


Figure 6g.

AAL587 Simulator Match: Load Factors

Yaw Damper Implementation Comparison

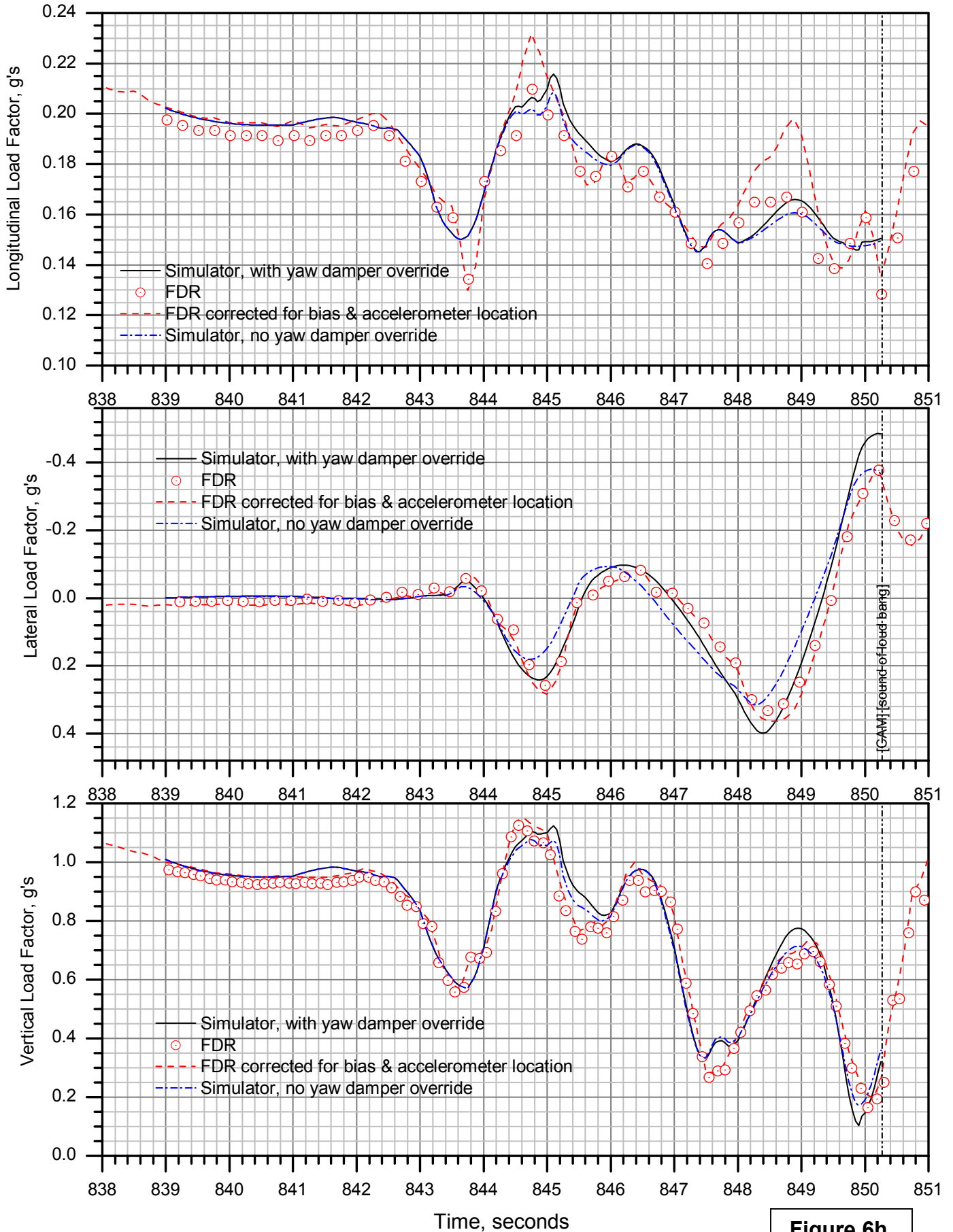


Figure 6h.

AAL587 Simulator Match: Altitude & Speed

Yaw Damper Implementation Comparison

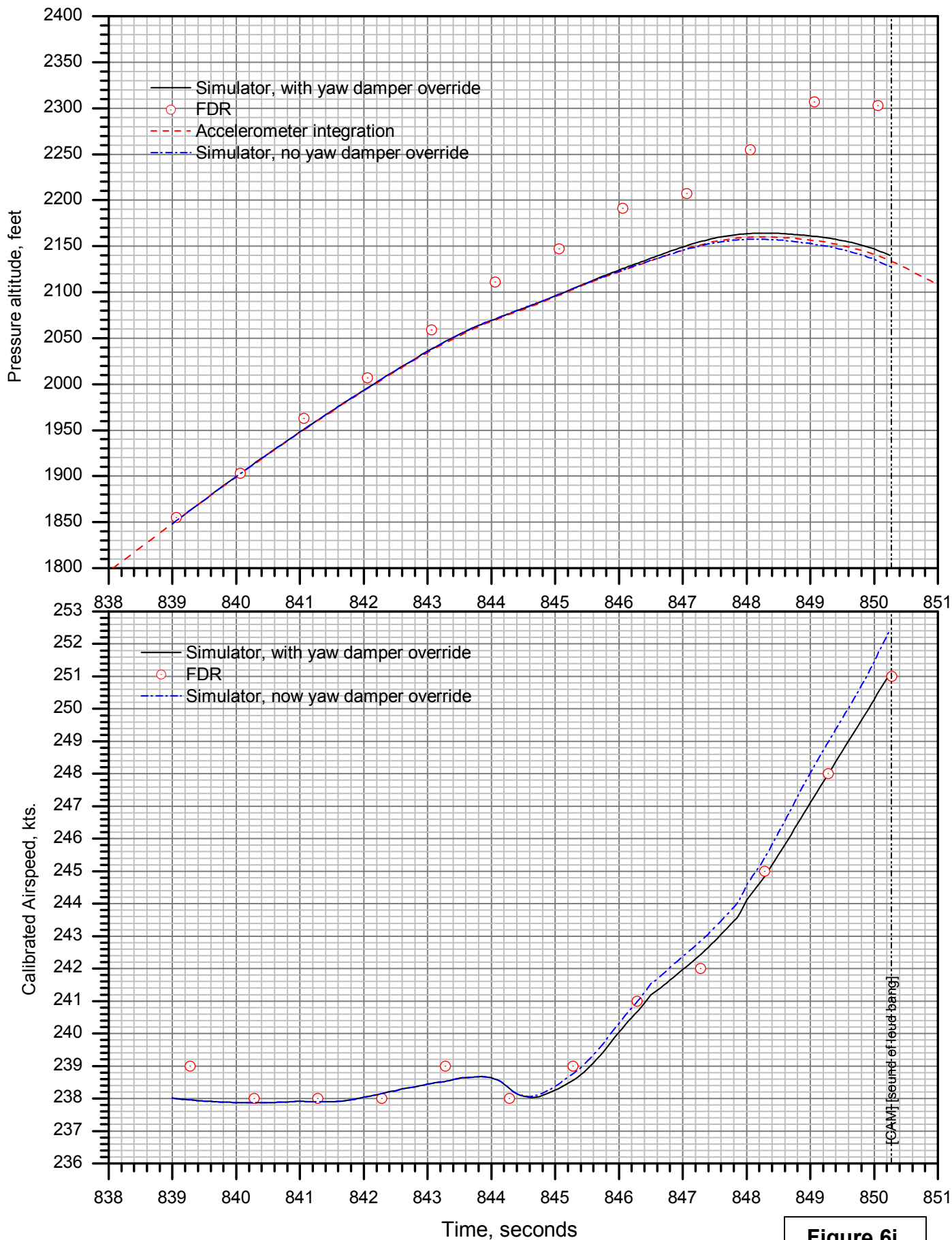


Figure 6i.

AAL 587 and JAL 47 Radar Tracks

